Quantum phase transitions of metals

Subir Sachdev
Department of Physics, Harvard University,
Cambridge, Massachusetts, 02138, USA
(Dated: July 10, 2024)

Lecture notes for
'Prospects in Theoretical Physics 2024',
Quantum Matter Summer School,
July 8-19, 2024.

Contains extracts from:

- *Quantum Phases of Matter*, by S. S., Cambridge University Press (2023).
- *Strange Metals and Black Holes: Insights From the Sachdev-Ye-Kitaev Model*, S. S., Oxford Research Encyclopedia in Physics, December 2023; arXiv:2305.01001

CONTENTS

I. FERMI LIQUID THEORY

The conventional theory of metals starts from a theory of the free electron gas, and then perturbatively accounts for the Coulomb interactions between the electrons. Already at leading order, we find a rather strong effect of the Coulomb interactions: a logarithmic divergence in the effective mass of the single-particle excitations near the Fermi surface. Further examination of the perturbation theory shows that this divergence of an artifact of failing to account for the screening of the long-range Coulomb interactions. Formally, screening can be accounted for by a simple modification of the perturbative series: introduce a dielectric constant in the interaction propagator, and sum only graphs which irreducible with respect to the interaction line. Once screening is accounted for by this method, the effective mass of the single-particle excitations becomes finite.

In this initial section we ask: is it possible to give a description of the interacting electron gas which is valid to all orders in the Coulomb interactions? By "all orders in perturbation theory" we are assuming the validity of perturbation theory, and cannot rule out non-perturbative effects which could lead to the appearance of new phases of matter. Indeed the study of such new phases of matter is the focus of a major part of this book. But in this chapter, we present an all-orders description of the electron gas. This starts by formalizing the definition of a "quasiparticle" excitation, as a central ingredient in the theory of many-particle quantum systems.

A. Free electron gas

Let us start by recalling the basic properties of the free electron gas. We work in a second quantized formalism with electron annihilation operators $c_{\boldsymbol{p}\alpha}$ where $\boldsymbol{p}$ is momentum and $\alpha = \uparrow, \downarrow$ is the electron spin. The electron operator obeys the anti-commutation relation

$$[c_{\boldsymbol{k}\alpha}, c^\dagger_{\boldsymbol{k}'\beta}]_+ = \delta_{\boldsymbol{k},\boldsymbol{k}'}\delta_{\alpha\beta} \tag{1}$$

We assume the dispersion of a single electron is $\varepsilon_{\boldsymbol{p}}$. The chemical potential is assumed to be included in $\varepsilon_{\boldsymbol{p}}$; so for the jellium model $\varepsilon_{\boldsymbol{p}} = \hbar^2\boldsymbol{p}^2/(2m) - \mu$. Then the Hamiltonian is

$$H = \sum_{\boldsymbol{p},\alpha} \varepsilon_{\boldsymbol{p}} c^\dagger_{\boldsymbol{p}\alpha} c_{\boldsymbol{p}\alpha} \,. \tag{2}$$

The $T = 0$ ground state of this Hamiltonian is

$$|G\rangle = \prod_{\varepsilon_{\boldsymbol{p}}<0,\alpha} c^\dagger_{\boldsymbol{p}\alpha}|0\rangle \tag{3}$$

The equation $\varepsilon_{\boldsymbol{p}} = 0$ defines the *Fermi surface* in momentum space, separating the occupied and unoccupied states.

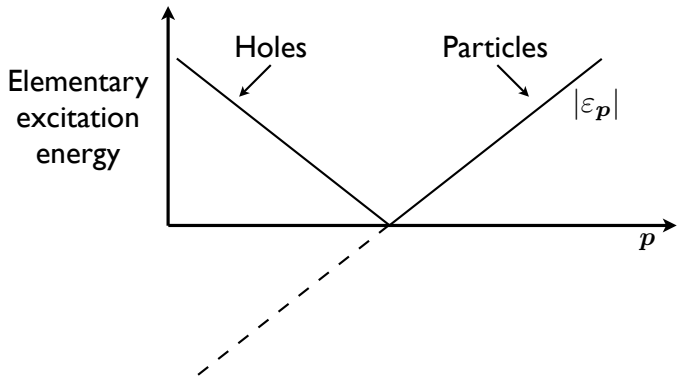

FIG. 1. Fermionic excitation spectrum of a Fermi liquid as a function of momentum $\boldsymbol{p}$ along a fixed direction from the origin.

The elementary excitations of this state are of two types. Outside the Fermi surface we have particle-like excitations

$$\underline{\text{Particles:}} \qquad c^\dagger_{\boldsymbol{p},\alpha}|G\rangle, \quad \boldsymbol{p} \text{ outside Fermi surface,} \tag{4}$$

while inside the Fermi surface we have hole-like excitations

$$\underline{\text{Holes:}} \qquad c_{\boldsymbol{p},\alpha}|G\rangle, \quad \boldsymbol{p} \text{ inside Fermi surface.} \tag{5}$$

The energy of these excitations must be positive (by definition), and is easily seen to equal $|\varepsilon_{\boldsymbol{p}}|$, as illustrated in Fig. 1.

From these elementary excitations, we can now build an exponentially large number of multi-particle and multi-particle excitations. In the free electron theory, their energies are simple the sum of the energies of the elementary excitations $\sum_{\boldsymbol{p},\alpha} |\varepsilon_{\boldsymbol{p}}|$.

B. Interacting electron gas

Our basic assumption is one of adiabatic continuity from the free electron gas. We imagine we can tune the strength of the Coulomb interactions, and slowly turn them on from the free electron theory. Alternatively, we can assert that there is no quantum phase transition as the strength of the interactions is increased: note this is an assumption, we will meet situations where this is not the case later. In this adiabatic process, we assume that there is a correspondence between the ground states and the elementary excitations of the free and interacting electron gas. So the state $|G\rangle$ in (3) evolves smoothly to the unknown ground state of the interacting electron gas. And importantly, there is also a correspondence in the excitations. In the 'jellium' model, with continuous translational symmetry and a uniform background neutralizing charge, this correspondence is simply one-to-one: a particle excitation with energy $\varepsilon_{\boldsymbol{p}}$ evolves into a 'quasiparticle excitation' with

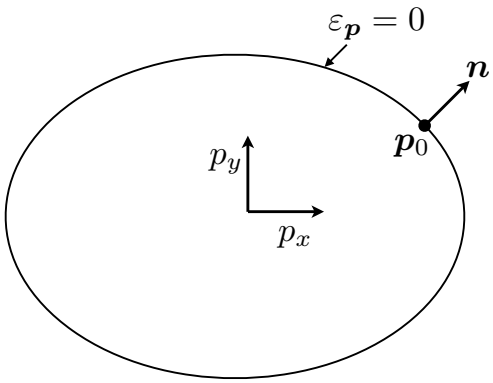

FIG. 2. A point $\boldsymbol{p}_0$ on the Fermi surface, and its unit normal $\boldsymbol{n}$.

a modified value of $\varepsilon_{\boldsymbol{p}}$. And similarly, for a 'quasihole' with modified energy $-\varepsilon_{\boldsymbol{p}}$. An important assumption will be that $\varepsilon_{\boldsymbol{p}}$ remains a smooth function through the Fermi surface, and the energies of both particles and holes is given by $|\varepsilon_{\boldsymbol{p}}|$.

In the presence of a lattice, the process of adiabatic evolution is more subtle, because we cannot assume that $\varepsilon_{\boldsymbol{p}}$ is only a function of $|\boldsymbol{p}|$. Consequently the *shape* of the Fermi surface can change in the adiabatic evolution, and a particle with momentum $\boldsymbol{p}$ can be inside the Fermi surface for the free electron gas, and outside the Fermi surface for the interacting electron gas. The crucial Luttinger theorem states that even though the shape of the Fermi surface can evolve, the volume enclosed by the Fermi surface is an adiabatic invariant; we discuss this theorem in Section I D. In the presence of a lattice, our basic assumption is that there is a smooth function $\varepsilon_{\boldsymbol{p}}$ so that the Fermi surface is defined by $\varepsilon_{\boldsymbol{p}} = 0$, and the excitation energies of the quasiparticles and quasiholes is $|\varepsilon_{\boldsymbol{p}}|$. Near, the Fermi surface, we assume a linear dependence in momentum orthogonal to the Fermi surface: at a point $\boldsymbol{p}_0$ on the Fermi surface, let the normal to the Fermi surface be the direction $\boldsymbol{n}$ (the value of p_F can depend upon $\boldsymbol{p}_0$, see Fig. 2), and so we can write for $\boldsymbol{p}$ close to $\boldsymbol{p}_0$

$$\varepsilon_{\boldsymbol{p}} = v_F(\boldsymbol{p} - \boldsymbol{p}_0) \cdot \boldsymbol{n}, \quad v_F = |\nabla_{\boldsymbol{p}} \varepsilon_{\boldsymbol{p}}| \equiv p_F/m^* \,, \tag{6}$$

where $p_F = |\boldsymbol{p}_0|$. This equation defines the Fermi momentum p_F, the Fermi velocity v_F, and the effective mass m^*, all of which can depend upon the direction $\hat{\boldsymbol{p}}_0$ in the presence of a lattice. Note that $\nabla_{\boldsymbol{p}} \varepsilon_{\boldsymbol{p}} = |\nabla_{\boldsymbol{p}} \varepsilon_{\boldsymbol{p}}| \boldsymbol{n}$ is a vector normal to the Fermi surface.

A further *assumption* in the theory of the interacting electron gas is that we can build up the exponentially large number of other excitations also be composing the elementary excitations. (In a finite system of size N, the number of elementary excitations is of order N, while the number of composite excitations is exponentially large in N.) As we are interested in the thermodynamic limit, we can characterize these excitations by the densities of quasiholes and quasiparticles. In practice, it is quite tedious to keep track of two separate densities, along with a non-analytic dependence of their excitation energy, $|\varepsilon_{\boldsymbol{p}}|$ on $\boldsymbol{p}$. Both these problems can be overcome by a clever

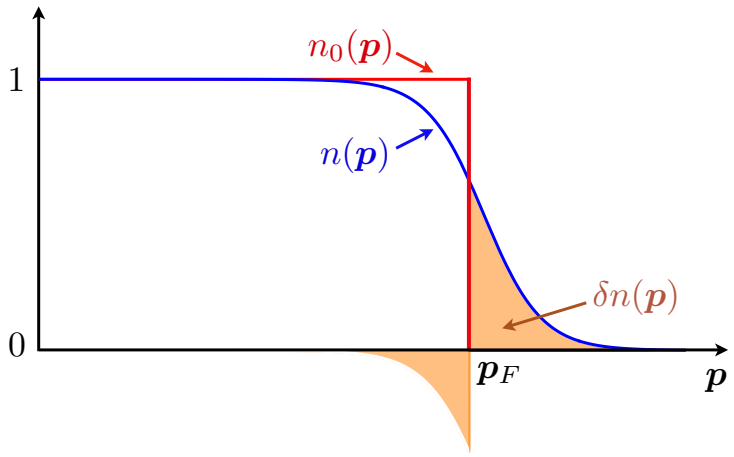

FIG. 3. Plot of the quasiparticle distribution functions $n(\boldsymbol{p})$ and $\delta n(\boldsymbol{p})$ of an excited state of the Fermi liquid. Note that $\delta n(\boldsymbol{p})$ has a discontinuity of unity at the Fermi surface.

mathematical trick; we emphasize that there is no physics assumption involved in this trick—it is merely a bookkeeping device. We *postulate* that the interacting ground state has the same form as the free electron ground state in (3). So the ground state has a density of quasiparticles $n_0(\boldsymbol{p})$ given by

$$\begin{aligned} n_0(\boldsymbol{p}) &= 1, \quad \boldsymbol{p} \text{ inside the Fermi surface} \\ n_0(\boldsymbol{p}) &= 0, \quad \boldsymbol{p} \text{ outside the Fermi surface} \end{aligned} \tag{7}$$

as shown in Fig. 3. Then, an excited state is characterized by density of quasiparticles $n(\boldsymbol{p})$, but the excitation energy will depend only upon

$$\delta n(\boldsymbol{p}) = n(\boldsymbol{p}) - n_0(\boldsymbol{p}), \tag{8}$$

where $\delta n(\boldsymbol{p})$ has a discontinuity of unity at the Fermi surface. So for $\boldsymbol{p}$ outside the Fermi surface $\delta n(\boldsymbol{p})$ measures the density of quasiparticle excitations, while for $\boldsymbol{p}$ inside the Fermi surface $-\delta n(\boldsymbol{p})$ measures the density of quasihole excitations. (All of these densities can also depend upon the spin of the quasiparticles or quasiholes, a complication we shall ignore in the following discussion.) So the actual density of excitations with energy $|\varepsilon_{\boldsymbol{p}}|$ is $|\delta n(\boldsymbol{p})|$. For the total excitation energy, which depends on their product, we can drop the absolute value: this is one of the advantages of this mathematical trick.

We assume we are at temperature $T \ll E_F$, so that the density of quasiparticles and quasiholes is small. Our first thought would be that because of the low density, we can ignore the interactions between the quasiparticles and quasiholes, and compute the total energy of the multiparticle/hole excitations simply by adding their individual energies. An important observation by Landau was that this is not correct. If we wish to work consistently to order $(T/E_F)^2$ in the total energy,

one (and only one) additional term is necessary; ignoring spin-dependence, we present the Landau energy functional

$$E[\delta n(\boldsymbol{p})] = \sum_{\boldsymbol{p}} \varepsilon_{\boldsymbol{p}} \delta n(\boldsymbol{p}) + \frac{1}{2V} \sum_{\boldsymbol{p},\boldsymbol{k}} F_{\hat{\boldsymbol{p}},\hat{\boldsymbol{k}}}\, \delta n(\boldsymbol{p}) \delta n(\boldsymbol{k})\,, \tag{9}$$

where V is the volume of the system. At a temperature $T \ll E_F$, $\delta n(\boldsymbol{p})$ is of order unity only in a window of momenta with $v_F|p - p_F| \sim T$ where $|\varepsilon_{\boldsymbol{p}}| \sim T$. Then, as we perform the radial integral in the first term in (3), we pick up a factor T from ε_p, and a second factor of T from the limits on the integral: so the first term is of order T^2. Landau's point is that the second term in (9) is also of order T^2: there now are 2 integrals over radial momenta, and their product yields a factor of T^2. This term describes the interaction between the quasiparticles and quasiholes, and is characterized by the unknown Landau interaction function $F_{\hat{\boldsymbol{p}},\hat{\boldsymbol{k}}}$. To order T^2, we can consistently assume that all the quasiparticles and quasiholes are practically on the Fermi surface in the interaction term, and so $F_{\hat{\boldsymbol{p}},\hat{\boldsymbol{k}}}$ depends only upon the directions of $\boldsymbol{p}$ and $\boldsymbol{k}$.

Although the quasiparticles and quasiholes are assumed to interact in Landau's functional, the interaction is conservative: *i.e.* it does not scatter quasiparticles between momenta, and change the quasiparticle distribution function. The main effect of the interaction term is that the change in the energy of the system upon adding a quasiparticle or quasihole depends upon the density of excitations already present. We will consider scattering processes of quasiparticles later in Section I C: these lead to a finite quasiparticle lifetime, but the correponding corrections to the energy functional are higher order in T.

Landau's central point is that the values of m^* and $F_{\hat{\boldsymbol{p}},\hat{\boldsymbol{k}}}$ are sufficient to provide a description of the low temperature properties of the interacting electron gas to order $(T/E_F)^2$, and all orders in the strength of the underlying Coulomb interactions.

C. Green's functions and quasiparticle lifetime

For further discussion of the properties of the Fermi liquid, and the nature of its corrections when we consider higher temperatures, it is useful to employ the language of Green's functions. We use the standard many-body Green's function defined in Ref. [1]. The most convenient definition starts from the Green's functions defined in imaginary time τ (ignoring the electron spin α)

$$G(\boldsymbol{p},\tau) = -\left\langle T_\tau c_{\boldsymbol{p}}(\tau) c^\dagger_{\boldsymbol{p}}(0)\right\rangle \tag{10}$$

where T_τ is the time-ordering symbol. We can then Fourier transform this to the Matsubara frequencies $\omega_n = (2n+1)\pi T/\hbar$, n integer, to obtain $G(\boldsymbol{p}, i\omega_n)$. More generally, we can consider the Green's function in the complex z plane, $G(\boldsymbol{p}, z)$, obtained by analytic continuation of $G(\boldsymbol{p}, i\omega_n)$. This Green's function obeys the spectral representation

$$G(\boldsymbol{p}, z) = \int_{-\infty}^{\infty} d\Omega\, \frac{\rho(\boldsymbol{p},\Omega)}{z - \Omega} \tag{11}$$

where $\rho(\boldsymbol{p},\Omega) = -(1/\pi)\mathrm{Im}\left[G(\boldsymbol{p},\Omega+i0^+)\right] > 0$ is the spectral density. We will also refer to the retarded Green's function $G^R(\boldsymbol{p},\omega) = G(\boldsymbol{p},\omega+i0^+)$, and more generally $G^R(\boldsymbol{p},z) = G(\boldsymbol{p},z)$ for z in the upper-half plane. Closely associated is the electron self-energy $\Sigma(\boldsymbol{p},z)$, which is related to the Green's function by Dyson's equation

$$G(\boldsymbol{p},z) = \frac{1}{z-\varepsilon^0_{\boldsymbol{p}}-\Sigma(\boldsymbol{p},z)} \tag{12}$$

where by $\varepsilon^0_{\boldsymbol{p}}$ we now denote the bare electron dispersion before the effects of electron-electron interactions are accounted for.

The postulates of Fermi liquid theory described above have strong implications for the structure of the Green's function in the complex frequency plane. Specifically, the existence of long-lived quasiparticles near the Fermi surface implies that the Green's function has a pole very close to the real frequency axis, at a frequency obeying $\mathrm{Re}(z) = \varepsilon_{\boldsymbol{p}}$ for $\boldsymbol{p}$ close to the Fermi surface. The existence of such a pole implies a free particle behavior of the Green's function at long times, representing the propagation of the quasiparticle. In this section, we wish to go beyond Fermi liquid theory and include a finite quasiparticle lifetime by taking the pole just off the real axis.

Actually, there is an important subtlety in the statement "there is a pole in the Green's function" that we need to keep in mind. The spectral definition (11) implies that $G(\boldsymbol{p},z)$ is an analytic function for all z, with a branch cut on the real frequency axis, for an interacting system with a reasonably smooth spectral density $\rho(\boldsymbol{p},\Omega)$. The pole is actually in a different Riemann sheet from the definition (11), and is reached by analytically continuing across the branch cut. So the retarded Green's function $G^R(\boldsymbol{p},z)$ is analytic for all z in the upper-half plane, and the pole is obtained when we analytically continue $G^R(\boldsymbol{p},z)$ to the lower-half plane (where it is *not* equal to the $G(\boldsymbol{p},z)$ defined by (11)). For $\boldsymbol{p}$ close to the Fermi surface in a Fermi liquid, this pole is at a frequency $z = \varepsilon_{\boldsymbol{p}} - i\gamma_{\boldsymbol{p}}$ where $\gamma_{\boldsymbol{p}} > 0$ is related to the quasiparticle lifetime $\tau_{\boldsymbol{p}} = 1/(2\gamma_{\boldsymbol{p}})$ because it leads to exponential decay for the Green's function in real time (the factor of 2 arises because we measure the *probability* of observing a quasiparticle a time $\tau_{\boldsymbol{p}}$ after creating it). Note that the pole is in the lower-half plane of the analytically continued $G^R(\boldsymbol{p},z)$ for both signs of $\varepsilon_{\boldsymbol{p}}$ *i.e.* for both quasiparticles and quasiholes: see Fig. 4.

Ultimately, this complexity can be succinctly captured by initially restricting attention to the G Green's function on the imaginary frequency axis. Then, the existence of the quasiparticle implies that the Green's function defined by (11) obeys

$$G(\boldsymbol{p},i\omega) = \frac{Z_{\hat{\boldsymbol{p}}}}{i\omega-\varepsilon_{\boldsymbol{p}}+i\gamma_{\boldsymbol{p}}\,\mathrm{sgn}(\omega)} + G_{\mathrm{inc}}(\boldsymbol{p},i\omega_n)\,, \tag{13}$$

where $\varepsilon^0_{\boldsymbol{p}}$ is the 'bare' electron dispersion,

$$\varepsilon_{\boldsymbol{p}} = \varepsilon^0_{\boldsymbol{p}} + \mathrm{Re}\left[\Sigma(\boldsymbol{p},0)\right] \tag{14}$$

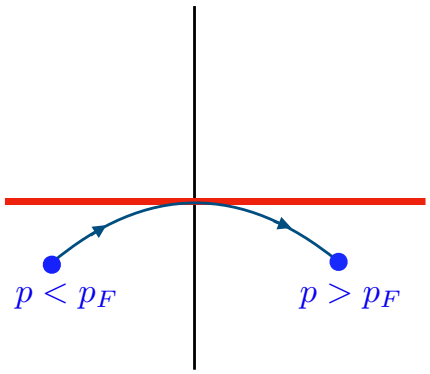

FIG. 4. The poles of the Green's function $G^R(\boldsymbol{p}, z)$ in the complex z plane. The poles are in the second Riemann sheet, and the horizontal line represents the branch cut implied by (11).

is the 'renormalized' quasiparticle dispersion, and

$$\gamma_{\boldsymbol{p}} = -\mathrm{Im}\left[\Sigma(\boldsymbol{p}, \varepsilon_{\boldsymbol{p}} + i0^+)\right] > 0\,. \tag{15}$$

Consistency of the above definitions requires that the inverse lifetime of the quasiparticle is much smaller than its excitation energy, *i.e.*

$$\gamma_{\boldsymbol{p}} \ll |\varepsilon_{\boldsymbol{p}}|\,, \tag{16}$$

for $\boldsymbol{p}$ close the Fermi surface. The Fourier transform of G has a slowly-decaying contribution which is just that of a free particle but with renormalized dispersion, and an amplitude suppressed by $Z_{\hat{\boldsymbol{p}}}$. Consequently, $Z_{\hat{\boldsymbol{p}}}$ is the quasiparticle residue, and it equals the square of the overlap between the free and quasiparticle wavefunctions. The G_{inc} term is the 'incoherent' contribution, associated with additional excitations created from the particle-hole continuum upon inserting a single particle into the system: this contribution decays rapidly in time, and can be ignored relative the quasiparticle contribution for the low energy physics.

From (13), we can now compute the momentum distribution function $n_e(\boldsymbol{p})$ of the underlying electrons;

$$n_e(\boldsymbol{p}) = \left\langle c^\dagger_{\boldsymbol{p}} c_{\boldsymbol{p}} \right\rangle\,, \tag{17}$$

where we are dropping the spin index. For a free electron gas

$$n_e(\boldsymbol{p}) = \theta(-\varepsilon^0_{\boldsymbol{p}}), \quad \text{free electrons, } T = 0, \tag{18}$$

where $\theta(x)$ is the unit step function. So there is a discontinuity of size unity on the Fermi surface in $n_e(\boldsymbol{p})$. For the interacting electron gas, it is important to distinguish $n_e(\boldsymbol{p})$ from the distribution function of quasiparticles $n(\boldsymbol{p})$ in (8). The *quasiparticle* momentum distribution function continues to have a discontinuity of size *unity* on the Fermi surface $\varepsilon_{\boldsymbol{p}} = 0$. For the electron momentum

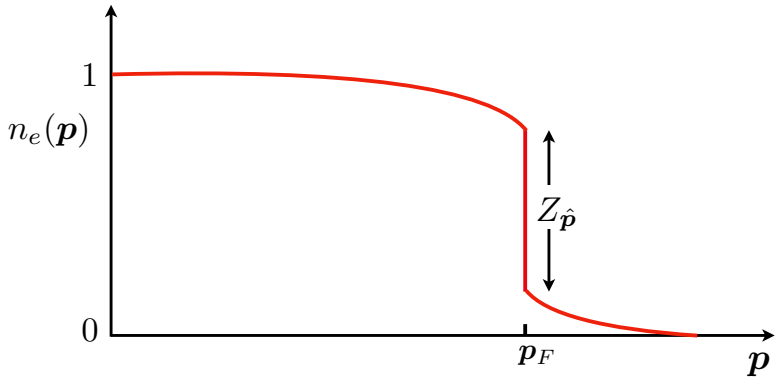

FIG. 5. The momentum distribution function of bare electrons in a Fermi liquid at $T = 0$. There is a discontinuity of size $Z_{\hat{\boldsymbol{p}}}$ on the Fermi surface.

distribution function at $T = 0$, we need to evaluate

$$n_e(\boldsymbol{p}) = \int_{-\infty}^{\infty} \frac{d\omega}{2\pi} G(\boldsymbol{p}, i\omega) e^{i\omega 0^+} \tag{19}$$

Evaluating the integral in (19) using (13), we find a discontinuous contribution from the pole near the Fermi surface. There is no reason to expect a discontinuity from $G_{\rm inc}$, and so we obtain

$$n_e(\boldsymbol{p}) = Z_{\hat{\boldsymbol{p}}}\, \theta(-\varepsilon_{\boldsymbol{p}}) + \ldots, \quad \text{interacting electrons, } T = 0, \tag{20}$$

where $\ldots$ is the contribution from $G_{\rm inc}$. We show a typical plot of $n_e(\boldsymbol{p})$ in Fig. 5. Because $n_e(\boldsymbol{p})$ must be positive and bounded by unity, we have a constraint on the quasiparticle residue

$$0 < Z_{\hat{\boldsymbol{p}}} \leq 1\,. \tag{21}$$

Note that a small $Z_{\hat{\boldsymbol{p}}}$ is not an indication that the Fermi liquid theory is not robust: it merely indicates a small overlap between the bare electron and the renormalized quasiparticle. Systems with very small $Z_{\hat{\boldsymbol{p}}}$ can be very good Fermi liquids: the heavy-fermion compounds discussed in Section V are of this type. Rather it is a short quasiparticle lifetime, or large $\gamma_{\boldsymbol{p}}$, and the failure of (16), which is a diagnostic of the breakdown of Fermi liquid theory. We will turn to 'non-Fermi liquids' (which also have $Z_{\hat{\boldsymbol{p}}} = 0$) in Section VII.

For an explicit evaluation of the inverse lifetime $\gamma_{\boldsymbol{p}}$, we have to consider processes beyond those present in Landau Fermi liquid theory. In particular, we have to evaluate the imaginary part of the self energy in (15) for $\boldsymbol{p}$ near the Fermi surface. This requires a somewhat tedious evaluation of the relevant Feynman diagrams, and we will explicitly compute an example in Section VII A. For now, we will be satisfied here by 'guessing' the answer by Fermi's golden rule. Assuming only

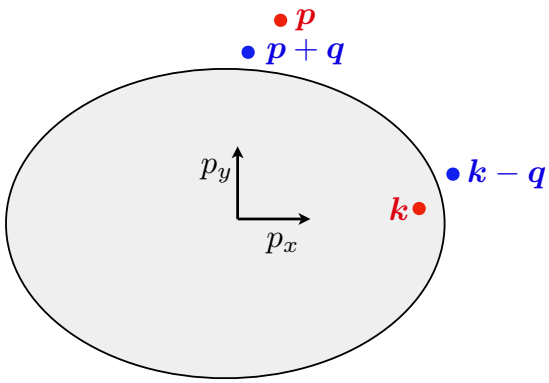

FIG. 6. Decay of a quasiparticle with momentum $\boldsymbol{p}$ by scattering off a pre-existing quasiparticle with momentum $\boldsymbol{k}$ to produce a quasiparticles of momena $\boldsymbol{p}+\boldsymbol{q}$ and $\boldsymbol{k}-\boldsymbol{q}$.

a contact interaction, U, between the quasiparticles, we can write down the inverse lifetime

$$\frac{1}{\tau_{\boldsymbol{p}}} = 2\gamma_{\boldsymbol{p}} = 2\pi U^2 \frac{1}{V^2} \sum_{\boldsymbol{k},\boldsymbol{q}} f(\varepsilon_{\boldsymbol{k}})[1-f(\varepsilon_{\boldsymbol{p}+\boldsymbol{q}})][1-f(\varepsilon_{\boldsymbol{k}-\boldsymbol{q}})] \times \delta\left(\varepsilon_{\boldsymbol{p}}+\varepsilon_{\boldsymbol{k}}-\varepsilon_{\boldsymbol{p}+\boldsymbol{q}}-\varepsilon_{\boldsymbol{k}-\boldsymbol{q}}\right) . \tag{22}$$

This obtained by employing Fermi's golden role to the process sketched in Fig. 6, and including probabilities that the initial states are occupied, and the final states are empty. The momentum integrals in (22) are quite difficult to evaluate in general, but it is not difficult to see that the result becomes very small for $\boldsymbol{p}$ near the Fermi surface and small T, because of the constraints imposed by the Fermi functions and the energy conserving delta function. A simple overestimate can be made by simply ignoring the constraints from momentum conservation, in which case we obtain

$$\begin{aligned}\gamma_\varepsilon &\sim U^2[d(0)]^3 p_F^{-d} \int_{-\infty}^{\infty} d\varepsilon_1 d\varepsilon_2 d\varepsilon_3 f(\varepsilon_1)[1-f(\varepsilon_2)][1-f(\varepsilon_3)] \\ &\qquad \times \delta(\varepsilon+\varepsilon_1-\varepsilon_2-\varepsilon_3) \\ &= U^2[d(0)]^3 p_F^{-d} \times \begin{cases} \pi^2 T^2/4 & \text{for } \varepsilon = 0 \\ \varepsilon^2/2 & \text{for } T = 0\,. \end{cases}\end{aligned} \tag{23}$$

More careful considerations of momentum conservations are needed to obtain the precise coefficients (see Section VII A for an example), but they show that the power-laws above in T and ε are correct. So at low temperatures, $\gamma_{\boldsymbol{p}} \sim T^2$ is always much smaller than $|\varepsilon_{\boldsymbol{p}}| \sim T$, and this justifies Fermi liquid theory.

We can also use these results to give a formal definition of the Fermi surface using Green's functions. Notice that γ_ε in (23) vanishes as $\varepsilon \to 0$ at $T = 0$. This follows from the vanishing of the phase space for the decay of an excitation with energy ε as $\varepsilon \to 0$. This is actually a special case of a more general phenomenon following from the stability of the ground state, and does not

even require excitations to be close to the Fermi surface. The more general statement is

$$\text{Im}\left[\Sigma(\boldsymbol{p}, \Omega + i0^+)\right] \to 0 \text{ as } \Omega \to 0 \text{ at } T = 0 \tag{24}$$

for any $\boldsymbol{p}$, and its validity can be checked by examining the structure of the Feynman graph expansion for Σ. We will see in Section VII B that (24) applies also to non-Fermi liquids without quasiparticle excitations. We can now define the Fermi surface by the pole in the Green's function which is determined by

$$G^{-1}(\boldsymbol{p}_F, i0^+) = 0 \text{ at } T = 0. \tag{25}$$

By (24), the left hand side of (25) is real, and so the solution of (25) determines a surface of co-dimension 1 in $\boldsymbol{p}$ space, which is the Fermi surface. These definitions will be useful in establishing the Luttinger relation constraining the volume enclosed by the Fermi surface, which we will discuss next in Section I D.

D. The Luttinger relation

We will present a proof of the Luttinger relation following the classic text book treatments, but will use an approach which highlights its connections to the modern developments. Specifically, there is a fundamental connection between the Luttinger relation and U(1) symmetries [2, 3]: any many body quantum system has a Luttinger relation associated with each U(1) symmetry, and this connects the density of the U(1) charge in the ground state to the volume enclosed by its Fermi surfaces. This relation applies both to systems of fermions and bosons, or of mixtures of fermions and bosons. However, the relation does not apply if the U(1) symmetry is 'broken' or 'Higgsed' by the condensation of a boson carrying the U(1) charge. As bosons are usually condensed at low temperatures, the Luttinger relation is not often mentioned in the context of bosons. However, there can be situations when bosons do not condense *e.g.* if the bosons bind with fermions to form a fermionic molecule, and then the molecules form a Fermi surface: then we will have to apply the Luttinger relation to the boson density [2].

We begin by noting a simple argument on why there could even be a relation between a short time correlator (the density, given by an 'ultraviolet' (UV) equal-time correlator) and a long-time correlator (the Fermi surface is the locus of zero energy excitations in a Fermi liquid, an 'infrared' (IR) property). In the fermion path integral, the free particle term in the Lagrangian is

$$\mathcal{L}_c^0 = \sum_{\boldsymbol{p}} c_{\boldsymbol{p}}^\dagger \left(\frac{\partial}{\partial \tau} + \varepsilon_{\boldsymbol{p}}^0 - \mu \right) c_{\boldsymbol{p}}, \tag{26}$$

where we have now chosen to extract the chemical potential μ explicitly from the bare dispersion $\varepsilon_{\boldsymbol{p}}^0$. The expression in (26) is invariant under global U(1) symmetry

$$c_{\boldsymbol{p}} \to c_{\boldsymbol{p}} e^{i\theta} \quad , \quad c_{\boldsymbol{p}}^\dagger \to c_{\boldsymbol{p}}^\dagger e^{-i\theta} \tag{27}$$

as are the rest of the terms in the Lagrangian describing the interactions between the electrons. However, let us now 'gauge' this global symmetry by allowing θ to have a *linear* dependence on imaginary time τ:

$$c_{\boldsymbol{p}} \to c_{\boldsymbol{p}} e^{\mu\tau} \quad , \quad c^\dagger_{\boldsymbol{p}} \to c^\dagger_{\boldsymbol{p}} e^{-\mu\tau} \tag{28}$$

Note that in the Grassman path integral, $c_{\boldsymbol{p}}$ and $c^\dagger_{\boldsymbol{p}}$ are independent Grassman numbers and so the two transformations in (28) are not inconsistent with each other. The interaction terms in the Lagrangian are explicitly invariant under the time-dependent U(1) transformation in (28). The free particle Lagrangian in (26) is not invariant under (28) because of the presence of the time derivative term; however, application of (28) shows that μ cancels out of the transformed $\mathcal{L}^0_c$, and so has completely dropped out of the path integral. We seem to have reached the absurd conclusion that the properties of the electron system are independent of μ: this is explicitly incorrect even for free particles.

What is wrong with the above argument which 'gauges away' μ by the transformation in (28)? The answer becomes clear from the expression for the total electron density

$$\rho_e = \frac{1}{V} \sum_{\boldsymbol{p}} \int_{-\infty}^{\infty} \frac{d\omega}{2\pi} G(\boldsymbol{p}, i\omega) e^{i\omega 0^+} \, . \tag{29}$$

The transformation in (28) corresponds to a shift in frequency $\omega \to \omega + i\mu$ of the contour of integration, and this is not permitted because of singularities in $G(\boldsymbol{p}, i\omega)$. However, as show below, it is possible to manipulate (29) into a part which contains the full answer, and a remainder which vanishes because manipulations similar to the failed frequency shift in (28) become legal.

The key step to extracting the non-zero part is to use the following simple identity which follows directly from Dyson's equation (12)

$$\begin{aligned} G(\boldsymbol{p}, i\omega) &= G_{ff}(\boldsymbol{p}, i\omega) + G_{LW}(\boldsymbol{p}, i\omega) \\ G_{ff}(\boldsymbol{p}, i\omega) &\equiv i \frac{\partial}{\partial \omega} \ln \left[G(\boldsymbol{p}, i\omega) \right] \\ G_{LW}(\boldsymbol{p}, i\omega) &\equiv -i G(\boldsymbol{p}, i\omega) \frac{\partial}{\partial \omega} \Sigma(\boldsymbol{p}, i\omega) \, . \end{aligned} \tag{30}$$

The non-zero part is G_{ff}: it is a frequency derivative, and so its frequency integral in (29) is not difficult to evaluate exactly after carefully using the $e^{i\omega 0^+}$ convergence factor. The subscript of G_{ff} denotes that this the only term which is non-vanishing for free fermions; indeed we will see below that the frequency integral of G_{ff} has the same value for interacting fermions as for free fermions with the same Fermi surface. The remaining contribution from G_{LW} vanishes for free particles (which have vanishing Σ). Therefore, establishing the Luttinger relation, *i.e.* the invariance of the volume enclosed by the Fermi surface, reduces then to establishing that the contribution of G_{LW} to (29) vanishes.

We consider the latter important step first. We would like to show that

$$\sum_{\boldsymbol{p}} \int_{-\infty}^{\infty} \frac{d\omega}{2\pi} G_{LW}(\boldsymbol{p}, i\omega) = 0\,. \tag{31}$$

We now show that (31) follows from the transformations of G_{LW} under the gauge transformation in (28) for an imaginary chemical potential

$$c_{\boldsymbol{p}} \to c_{\boldsymbol{p}} e^{+i\omega_0 \tau} \quad , \quad c^\dagger_{\boldsymbol{p}} \to c^\dagger_{\boldsymbol{p}} e^{-i\omega_0 \tau}\,. \tag{32}$$

The argument relies on the existence of a functional, $\Phi_{LW}\left[G(\boldsymbol{p}, i\omega)\right]$, of the Green's function, called the Luttinger-Ward functional, so that the self energy is its functional derivative

$$\Sigma(\boldsymbol{p}, i\omega) = \frac{\delta \Phi_{LW}}{\delta G(\boldsymbol{p}, i\omega)}\,. \tag{33}$$

The existence of such a functional can be seen diagrammatically, in which the Luttinger-Ward functional equals the interaction dependent terms for the free energy written in a 'skeleton' graph expansion in terms of the fully renormalized Green's function. Taking the functional derivative with respect to $G(\boldsymbol{p}, \omega)$ is equivalent to cutting a single G from all such graphs in all possible ways, and these are just the graphs for the self energy. For a more formal argument, see Ref. [4]. An important property of the Luttinger-Ward functional is its invariance under frequency shifts

$$\Phi\left[G(\boldsymbol{p}, i\omega + i\omega_0)\right] = \Phi\left[G(\boldsymbol{p}, i\omega)\right]\,, \tag{34}$$

for any fixed ω_0. Here, we are regarding Φ as functional of two distinct functions $f_{1,2}(\omega)$, with $f_1(\omega) \equiv G(\boldsymbol{p}, i\omega + i\omega_0)$ and $f_2(\omega) = G(\boldsymbol{p}, i\omega)$, and Φ evaluates to the same value for these two functions. Now note that this frequency shift is nothing but the gauge transformation in (32); therefore (34) follows from the fact that such frequency shifts are allowed in Φ_{LW}. The singularity on the real frequency axis is sufficiently weak so that the frequency shifts are legal in a Fermi liquid; but we note that in the non-Fermi liquid SYK model to be considered in Section VI, the Green's functions are significantly more singular at $\omega = 0$, and the analogs of (31) and (34) do not apply. For the Fermi liquid, we can now expand (34) to first order in ω_0, using (33), and integrating by parts we establish (31).

Now that we have disposed of the offending term in (30), we can return to (29) and evaluate

$$\rho_e = \frac{i}{V} \sum_{\boldsymbol{p}} \int_{-\infty}^{\infty} \frac{d\omega}{2\pi} \frac{\partial}{\partial \omega} \ln\left[G(\boldsymbol{p}, i\omega)\right] e^{i\omega 0^+}\,. \tag{35}$$

We will evaluate the ω integral by distorting the contour in the frequency plane. For this, we need to carefully understand the analytic structure of the integrand. This is subtle, because there are two types of branch cuts. One branch cut arises from the Green's function: $G(\boldsymbol{p}, z)$ has a branch cut

along the real axis $\mathrm{Im}(z) = 0$, with $\mathrm{Im}G(\boldsymbol{p}, z) \leq 0$ for $\mathrm{Im}(z) = 0^+$, $\mathrm{Im}G(\boldsymbol{p}, z) \geq 0$ for $\mathrm{Im}(z) = 0^-$ and $\mathrm{Im}G(\boldsymbol{p}, z) = 0$ for $z = 0$. The other branch cut is from the familiar $\ln(z)$ function: we take this on the positive real axis, with a discontinuity of $2i\pi$. First, we account for the branch cut in $G(\boldsymbol{p}, z)$, by distorting the contour of integration in (35) to pick up the discontinuity $\mathrm{Im}G(\boldsymbol{p}, z)$

$$\rho_e = \frac{-i}{V} \sum_{\boldsymbol{p}} \int_{-\infty}^{0} \frac{dz}{2\pi} \frac{\partial}{\partial z} \ln \left[\frac{G(\boldsymbol{p}, z + i0^+)}{G(\boldsymbol{p}, z + i0^-)} \right] . \tag{36}$$

Note from (12) and (24) that on real frequency axis $\mathrm{Im}\, G(\boldsymbol{p}, z + i0^{\pm}) \to 0$ as $z \to 0$ or $-\infty$. Consequently the only possible values of $\ln[G(\boldsymbol{p}, z + i0^+)/G(\boldsymbol{p}, z + i0^-)]$ are $0, \pm 2\pi i$ as $z \to 0$ or $-\infty$, from the branch cut of the logarithm. So we obtain from (36)

$$\begin{aligned} \rho_e &= \frac{-i}{2\pi V} \sum_{\boldsymbol{p}} \ln \left[\frac{G(\boldsymbol{p}, i0^+)}{G(\boldsymbol{p}, i0^-)} \right] \\ &= \frac{1}{V} \sum_{\boldsymbol{p}} \theta \left(-\varepsilon^0_{\boldsymbol{p}} + \mu - \Sigma(\boldsymbol{p}, i0^+) \right) \\ &= \frac{1}{V} \sum_{\boldsymbol{p}} \theta \left(-\varepsilon_{\boldsymbol{p}} \right) , \end{aligned} \tag{37}$$

where we have used (14) and (24). Because the branch cut of the logarithm to extends to $z = +\infty$, only negative values of $\varepsilon_{\boldsymbol{p}}$ contribute to the z integral extending from $z = -\infty$ to $z = 0$. Eqn. (37) is the celebrated Luttinger relation, equating the electron density to the volume enclosed by the Fermi surface of the quasiparticles $\varepsilon_{\boldsymbol{p}} = 0$. In the presence of a crystalline lattice, there can be additional bands which are either fully filled or fully occupied: such bands will yield a contribution of unity or zero respectively to (37).

To summarize, the Luttinger relation is intimately connected to the U(1) symmetry of electron number conservation. Indeed, we can obtain a Luttinger relation for each U(1) symmetry of any system consisting of fermions or bosons. The result follows from the invariance of the Luttinger-Ward functional under the transformation in (32), in which we gauge the global symmetry to a linear time dependence: in this respect, there is a resemblance to 'tHooft anomalies in quantum field theories. If the U(1) symmetry is 'broken' by the condensation of a boson which carries U(1) charge, then the Luttinger relation no longer applies.

II. QUANTUM PHASE TRANSITION OF ISING QUBITS

$$H = -J \sum_{\langle ij \rangle} Z_i Z_j - Jg \sum_i X_i$$

$i \to$ d-dimensional hypercubic lattice

$X_i, Z_i \to$ Pauli operators :

$J > 0$, $g \geq 0$.

Determine phase diagram as a function of g.

Will find a quantum phase transition at

$g = g_c$ for all d.

(i) $g \gg 1$.

Unique ground state $|\rightarrow\rightarrow\rightarrow\rightarrow\cdots\rangle$.

"Quantum paramagnet" ; $|\rightarrow\rangle = \frac{1}{\sqrt{2}}(|\uparrow\rangle + |\downarrow\rangle)$

$|\leftarrow\rangle = \frac{1}{\sqrt{2}}(|\uparrow\rangle - |\downarrow\rangle)$

N-fold degenerate first excited states (N sites)

at $g = \infty$

$|i\rangle = |\rightarrow\rightarrow\rightarrow\leftarrow_i\rightarrow\rightarrow\rightarrow\cdots\rangle$

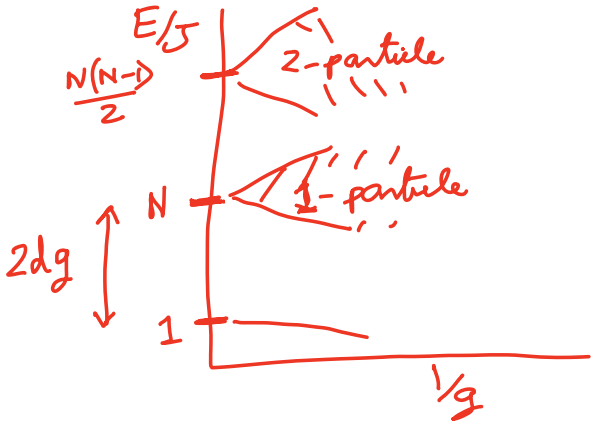

Use degenerate perturbation theory in $1/g$.

1- particle states

$$|\vec{k}\rangle = \frac{1}{\sqrt{N}} \sum_i e^{i\vec{k}\cdot\vec{r}_i} |i\rangle$$

$$\frac{\varepsilon_k}{J} = -Ng + 2g - 2\sum_{\alpha=1}^{d} \cos(k_\alpha a)$$

2- particle states

$$|\vec{k}_1, \vec{k}_2\rangle$$

Scattering and bound states...

(ii) $g \ll 1$

2- fold degenerate ferromagnetic ground states.

$$|\Uparrow\rangle = |\uparrow\uparrow\uparrow\uparrow\ldots\rangle$$

$$|\Downarrow\rangle = |\downarrow\downarrow\downarrow\downarrow\ldots\rangle$$

Cannot be smoothly connected to $g \gg 1$ at $N=\infty$

$\Rightarrow$ must be a quantum phase transition(s) at intermediate g

First excited states

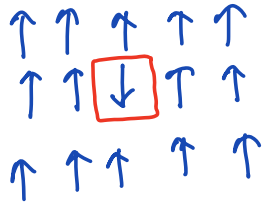

"Flipped spin" particle

$\varepsilon = 2dJ$

$d=1$ is special

Flipped spin "fractionalizes" into
2 domain-wall particles.

Dispersion of flipped spin particle:

Have to use effective Hamiltonian method
to perform perturbation theory to
order g^2.

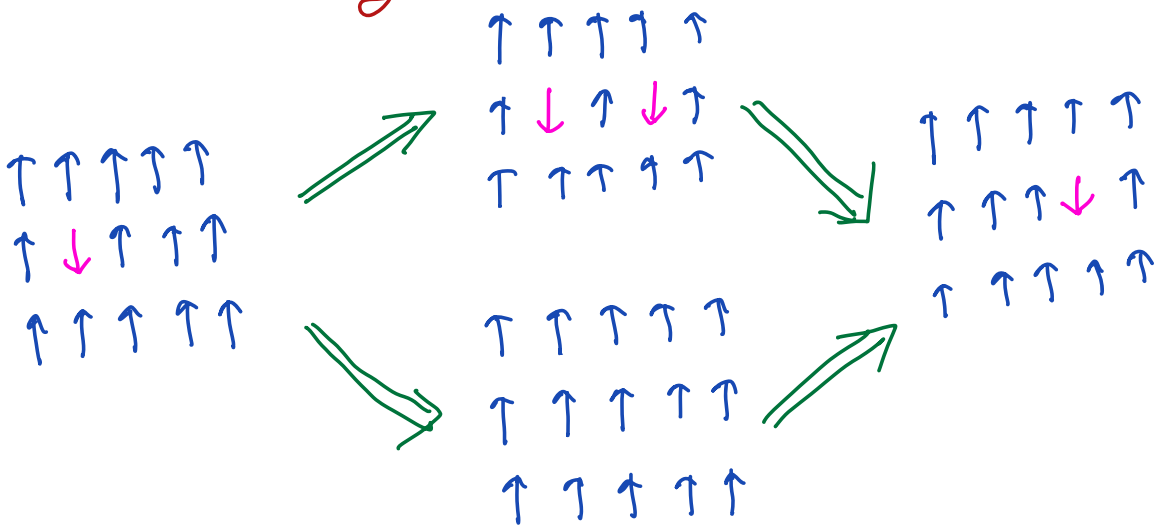

Total matrix element is zero unless initial and
final flipped spins are nearest neighbors.

$$\varepsilon_k = 2dJ + cJg^2 \sum_{\alpha=1}^{d} \cos(k_\alpha a)$$

Δ = gap to first excited state

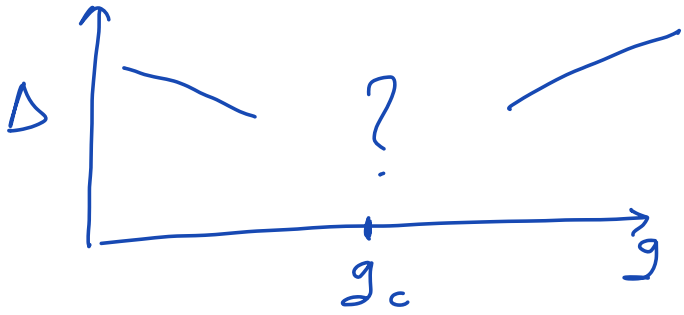

A single quantum phase transition at $g = g_c$ where Δ vanishes as

$$\Delta \sim |g - g_c|^{z\nu}$$

with $z = 1$.

Mapping to ϕ^4 quantum field theory

Consider the following non-linear oscillator

$$H = \frac{1}{2m} \Pi_\phi^2 + V(\phi)$$

$$[\phi, \Pi_\phi] = i$$

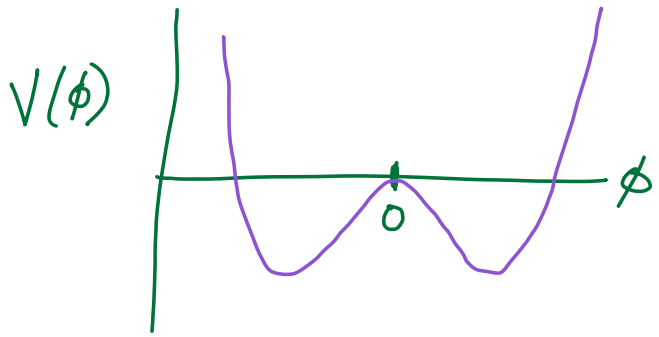

Focus on 2 lowest energy states

Tunneling under the barrier will lift the degeneracy and produce a gap Δ

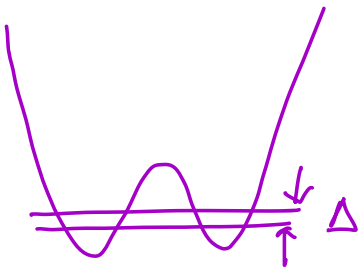

ground state

$$|\rightarrow\rangle = \frac{1}{\sqrt{2}}(\psi_U + \psi_D) \equiv \frac{1}{\sqrt{2}}(|\uparrow\rangle + |\downarrow\rangle)$$

$$|\leftarrow\rangle = \frac{1}{\sqrt{2}}(\psi_U - \psi_D) \equiv \frac{1}{\sqrt{2}}(|\uparrow\rangle - |\downarrow\rangle)$$

low energy Hamiltonian

$$H = -\frac{\Delta}{2} X$$

What is the operator ϕ in this low energy subspace ?

$$\phi|{\rightarrow}\rangle \Rightarrow \frac{\phi}{\sqrt{2}}\left(\psi_u(\phi)+\psi_D(\phi)\right)$$

π odd under $\phi \to -\phi$

$$\langle{\rightarrow}|\phi|{\rightarrow}\rangle = 0$$

$$\langle{\leftarrow}|\phi|{\leftarrow}\rangle = 0$$

$$\langle{\leftarrow}|\phi|{\rightarrow}\rangle = \int_{-\infty}^{\infty} d\phi \frac{\phi}{2}\left(\psi_u^*(\phi)-\psi_d^*(\phi)\right)\left(\psi_u(\phi)+\psi_d(\phi)\right)$$

$$= K \neq 0$$

$\Rightarrow$ ϕ maps to Z !

Now consider a lattice of such non-linear oscillators and couple them together

$$H = \sum_i \frac{1}{2m}\Pi_i^2 + \sum_i V(\phi_i) - \sum_{\langle ij\rangle} \tilde{J}\,\phi_i\,\phi_j$$

Provided the $\tilde{J}$ is not too-large, we can use the single-site mapping to obtain

$$\boxed{H_{eff} = -\frac{\Delta}{2}\sum_i X_i - \tilde{J}K^2 \sum_{\langle ij\rangle} Z_i Z_j}$$

From now on we will consider

$$H_\phi = \sum_i \frac{1}{2m} \Pi_{\phi_i}^2 + \sum_i \left(\frac{r}{2} \phi_i^2 + \frac{u}{24} \phi_i^4 \right)$$

$$- J \sum_{\langle ij \rangle} \phi_i \phi_j$$

In momentum space we can write

$$\phi_k = \frac{1}{\sqrt{N}} \sum_i \phi_i \, e^{i k r_i}$$

$$-J \sum_{\langle ij \rangle} \phi_i \phi_j = -J \sum_k |\phi_k|^2 \left(\sum_\alpha 2 \cos(k_\alpha a) \right)$$

$$\approx -2J \sum_k |\phi_k|^2 \left(2d - k^2 \ldots \right)$$

as $k \to 0$.

Now take the continuum limit while defining

$$\phi(x_i) = \frac{1}{\sqrt{a^d}} \phi_i$$

$$\Pi_\phi(x_i) = \frac{1}{\sqrt{a^d}} \Pi_{\phi_i}$$

so that

$$[\phi(x), \Pi_\phi(y)] = i \delta(x - y)$$

as $a \to 0$.

Then after various re-scalings

$$H_\phi = \int d^d x \left[\frac{1}{2} \Pi_\phi^2 + \frac{1}{2} (\vec{\nabla} \phi)^2 + \frac{r}{2} \phi^2 + \frac{u}{24} \phi^4 \right]$$

ϕ^4 quantum field theory!

Examine perturbation theory in u for $r<0$ and $r>0$.

i) $r>0$

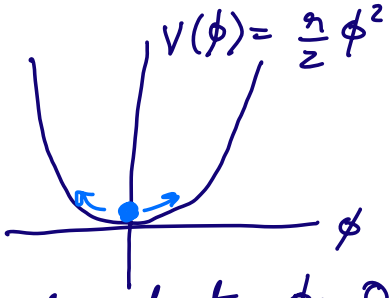

ϕ will fluctuate about $\phi = 0$.

$$H = \sum_k \left(\frac{\Pi_k^2}{2} + \frac{\phi_k^2}{2} (r + k^2) \right)$$

One oscillator for each k

$$\varepsilon_k = \sqrt{r + k^2}$$

Very similar to $g \gg 1$ Ising model

Gap vanishes as $r \searrow 0$

$$\Delta = \sqrt{r} \quad ; \quad z\nu = 1/2 .$$

(ii) $r < 0$

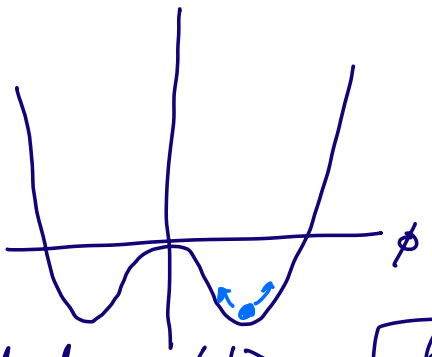

ϕ fluctuates about $\langle \phi \rangle = \sqrt{-\frac{6r}{u}}$

$$H_\phi = \sum_k \frac{|\phi_k|^2}{2}\left(2|r| + k^2\right) + \sum_k \frac{\pi_k^2}{2}$$

Similar to flipped spin quasiparticles at $g \ll 1$.

$$\varepsilon_k = \sqrt{k^2 + 2|r|}$$

Energy gap vanishes as

$$\Delta = \sqrt{2|r|}$$

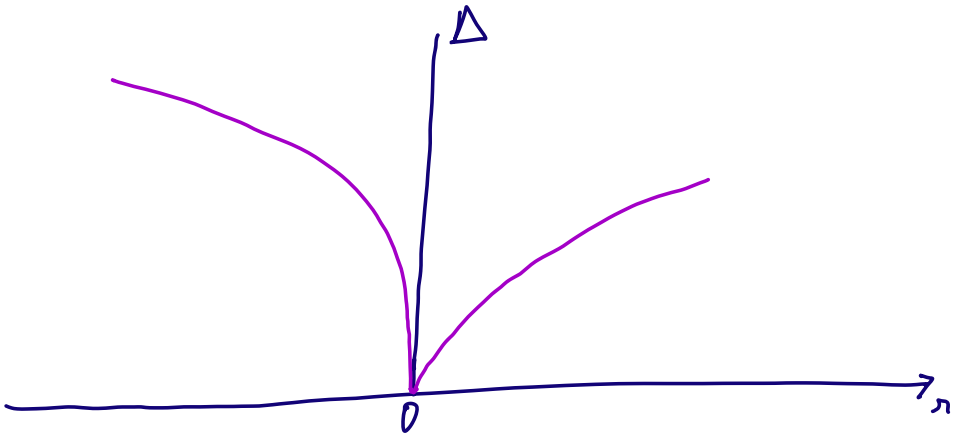

Quantum critical point at $r = 0$

$$\varepsilon_k = k$$

Massless relativistic boson

$$z = 1$$

Imaginary time path integral

Single particle path integral

$$H = \frac{m}{2}\Pi_\phi^2 + V(\phi)$$

$$Z = \mathrm{Tr}\, e^{-\beta H} = \int_{\phi(0)=\phi(\beta)} \mathcal{D}\phi(\tau)\, e^{-S[\phi]}$$

$$S[\phi] = \int_0^\beta d\tau \left[\frac{m}{2}\left(\frac{d\phi}{d\tau}\right)^2 + V(\phi)\right]$$

$$H_\phi = \int d^d x \left[\frac{1}{2}\Pi_\phi^2 + \frac{1}{2}(\nabla\phi)^2 + \frac{r}{2}\phi^2 + \frac{u}{24}\phi^4\right]$$

$$Z_\phi = \mathrm{Tr}\, e^{-\beta H_\phi} = \int_{\phi(x,\beta)=\phi(x,0)} \mathcal{D}\phi(x,\tau)\, \exp\left(-\int d^d x\, d\tau\, \mathcal{L}[\phi]\right)$$

$$\mathcal{L}[\phi] = \frac{1}{2}(\partial_t \phi)^2 + \frac{1}{2}(\nabla\phi)^2 + \frac{r}{2}\phi^2 + \frac{u}{24}\phi^4$$

$$= \frac{1}{2}(\partial_\mu \phi)^2 + \frac{r}{2}\phi^2 + \frac{u}{24}\phi^4$$

Relativistic quantum field theory in $d+1$ spacetime dimensions.

III. ISING FERROMAGNETISM IN A METAL

See slides at https://sachdev.physics.harvard.edu/UQM24QPTM.pdf.

We now consider the onset of Ising ferromagnetic order in a metal. This can be described by coupling the Z_i to the σ^z ferromagnetic moment of a Fermi liquid of electrons c_i. So we are led to consider the Hamiltonian

$$H = \sum_{\boldsymbol{k},\alpha} \varepsilon_{\boldsymbol{k}} c^\dagger_{\boldsymbol{k}\alpha} c_{\boldsymbol{k}\alpha} - J \sum_{\langle ij \rangle} Z_i Z_j - h \sum_i X_i - g \sum_i Z_i \, c^\dagger_{i\alpha} \sigma^z_{\alpha\beta} c_{i\beta} \tag{38}$$

(we have changed notation, and now use h for the transverse field, and g for the fermion-Ising 'Yukawa' coupling). Near the quantum phase transition for the onset of ferromagnetism, we can represent the quantum Ising model by a ϕ^4 quantum field theory, as in Section II, and obtain the continuum Lagrangian

$$\begin{aligned} \mathcal{L} = & \sum_{\boldsymbol{k},\alpha} c^\dagger_{\boldsymbol{k},\alpha} \left[\frac{\partial}{\partial \tau} + \varepsilon_{\boldsymbol{k}} \right] c_{\boldsymbol{k},\alpha} + \int d^2 r \left\{ \frac{1}{2} \left[(\boldsymbol{\nabla} \phi)^2 + (\partial_\tau \phi)^2 + s \, \phi^2 \right] + \frac{u}{4!} \phi^4 \right\} \\ & - \int d^2 r \, g \, \phi \, c^\dagger_\alpha \sigma^z_{\alpha\beta} c_\beta \end{aligned} \tag{39}$$

The Yukawa coupling g between ϕ and the fermions c is relevant, and we will consider its consequences in Section VII.

IV. SPIN DENSITY WAVE ORDER IN A METAL

See slides at https://sachdev.physics.harvard.edu/UQM24QPTM.pdf.

Let us now consider the onset of magnetism at a non-zero wavevector in a metal, often called a spin density wave (SDW). We will focus on the case where the wavevector of the SDW is $\boldsymbol{K} = (\pi, \pi)$ on the square lattice, and so the ordering has the same symmetry as the Néel state in an insulating antiferromagnet. The main ingredient here will be a bosonic collective mode representing antiferromagnetic spin fluctuations in the metal: this boson is the 'paramagnon'.

Near the transition from the Fermi liquid to the antiferromagnetic metal, it is possible to derive a systematic approach to the paramagnon modes of a metal. We begin with an electronic Hubbard model

$$H = \sum_{\boldsymbol{k},\alpha} \varepsilon_{\boldsymbol{k}} c^\dagger_{\boldsymbol{k}\alpha} c_{\boldsymbol{k}\alpha} + U \sum_i n_{i\uparrow} n_{i\downarrow} \tag{40}$$

where $n_{i\uparrow} \equiv c^\dagger_{i\uparrow} c_{i\uparrow}$, and similarly for $n_{i\downarrow}$. Upon using the single-site identity

$$U \left(n_{i\uparrow} - \frac{1}{2} \right) \left(n_{i\downarrow} - \frac{1}{2} \right) = - \frac{2U}{3} \boldsymbol{S}_i^2 + \frac{U}{4} \, , \tag{41}$$

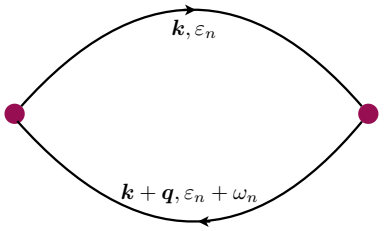

FIG. 7. Feynman diagram leading to (46).

(which is easily established from the electron commutation relations) it becomes possible to decouple the 4-fermion term in a particle-hole channel. We decouple the interaction term in the Hubbard model in (40), by the Hubbard-Stratonovich transformation

$$\exp\left(\frac{2U}{3}\sum_i \int d\tau \boldsymbol{S}_i^2\right) = \int \mathcal{D}\boldsymbol{\Phi}_i(\tau) \exp\left(-\sum_i \int d\tau \left[\frac{3}{8U}\boldsymbol{\Phi}_i^2 - \boldsymbol{\Phi}_i \cdot c_{i\alpha}^\dagger \frac{\boldsymbol{\sigma}_{\alpha\beta}}{2} c_{i\beta}\right]\right) \tag{42}$$

We now have a new field $\boldsymbol{\Phi}_i(\tau)$ which will play the role of the paramagnon field.

The path integral of the Hubbard model can now be written exactly as:

$$\mathcal{Z} = \int \mathcal{D}c_{i\alpha}(\tau)\mathcal{D}\boldsymbol{\Phi}_i(\tau) \exp\left(-\int d\tau \left\{\sum_{\boldsymbol{k},\alpha} c_{\boldsymbol{k}\alpha}^\dagger \left[\frac{\partial}{\partial\tau} + \varepsilon_{\boldsymbol{k}}\right] c_{\boldsymbol{k}\alpha} + \sum_i \left[\frac{3}{8U}\boldsymbol{\Phi}_i^2 - \boldsymbol{\Phi}_i \cdot c_{i\alpha}^\dagger \frac{\boldsymbol{\sigma}_{\alpha\beta}}{2} c_{i\beta}\right]\right\}\right). \tag{43}$$

We can now formally integrate out the electrons, and obtain

$$\frac{\mathcal{Z}}{\mathcal{Z}_0} = \int \prod_i \mathcal{D}\boldsymbol{\Phi}_i(\tau) \exp\left(-\mathcal{S}_{\text{paramagnon}}\left[\boldsymbol{\Phi}_i(\tau)\right]\right), \tag{44}$$

where $\mathcal{Z}_0$ is the free electron partition function. Close to the onset of SDW order (but still on the non-magnetic side), we can expand the action in powers of $\boldsymbol{\Phi}$

$$\mathcal{S}_{\text{paramagnon}}\left[\boldsymbol{\Phi}_i(\tau)\right] = \frac{T}{2}\sum_{\boldsymbol{q},\omega_n} |\boldsymbol{\Phi}(\boldsymbol{q},\omega_n)|^2 \left[\frac{3}{4U} - \frac{\chi_0(\boldsymbol{q}, i\omega_n)}{2}\right] + \ldots \tag{45}$$

where $\chi_0(\boldsymbol{q}, \omega_n)$ is the frequency-dependent Lindhard susceptibility, given by the particle-hole bubble graph shown in Fig. 7

$$\chi_0(\boldsymbol{q}, i\omega_n) = -\frac{T}{V}\sum_{\boldsymbol{p},\epsilon_n} \frac{1}{(i\epsilon_n - \varepsilon_{\boldsymbol{k}})(i\epsilon_n + i\omega_n - \varepsilon_{\boldsymbol{k}+\boldsymbol{q}})} \tag{46}$$

Performing the sum over frequencies by partial fractions, we obtain

$$\chi_0(\boldsymbol{q}, i\omega_n) = \frac{1}{V}\sum_{\boldsymbol{k}} \frac{f(\varepsilon_{\boldsymbol{k}+\boldsymbol{q}}) - f(\varepsilon_{\boldsymbol{k}})}{i\omega_n + \varepsilon_{\boldsymbol{k}} - \varepsilon_{\boldsymbol{k}+\boldsymbol{q}}}, \tag{47}$$

From the structure of the $\mathbf{\Phi}$ propagator, it is clear that $\mathbf{\Phi}$ will first condense at the wavevector $\boldsymbol{q}_{\rm max}$ at which $\chi_0(\boldsymbol{q}, i\omega = 0)$ is a maximum, and $\boldsymbol{q}_{\rm max}$ is then the wavevector of the SDW. In the mean field treatment of (45), the appearance of the this condensate requires that U is large enough to obey the 'Stoner criterion':

$$\frac{3}{4U} - \frac{\chi_0(\boldsymbol{q}_{\rm max}, i\omega = 0)}{2} < 0\,. \tag{48}$$

This wavevector is in turn determined by the dispersion $\varepsilon_{\boldsymbol{k}}$ of the underlying fermions. For simplicitly, we will only consider the case of a SDW with wavevector $\boldsymbol{K} = (\pi, \pi)$. The frequency dependence of $\chi_0(\boldsymbol{q}, i\omega)$ also has an important influence on the dynamics of the paramagnon fluctuations, related to the damping computed in Section VII for the Ising ferromagnetic case.

A. Fermi surface reconstruction

Let us now move into the antiferromagnetic metal phase, where there is a $\mathbf{\Phi}$ condensate at wavevector $\boldsymbol{K} = (\pi, \pi)$

$$\langle \mathbf{\Phi}_i \rangle = \eta_i \mathcal{N} \hat{\boldsymbol{z}}\,, \tag{49}$$

with $\mathcal{N}$ measuring the strength of the Néel ordered moment. We wish to describe the excitations of this state. One class of excitations are spin waves: these can be obtained by considering transverse fluctuations of $\mathbf{\Phi}$ about the condensate in (49) using the full action in (44). However, there are also low energy fermionic excitations in the antiferromagnetic metal, which are gapped in the insulator. We can determine the spectrum of the fermions by inserting (49) into the Yukawa coupling; using $\eta_i = e^{i\boldsymbol{K}\cdot\boldsymbol{r}_i}$, with $\boldsymbol{K} = (\pi, \pi)$, we can write the fermion Hamiltonian in momentum space

$$H_{\rm AFM} = \sum_{\boldsymbol{k}} \left[\varepsilon_{\boldsymbol{k}} c^\dagger_{\boldsymbol{k}\alpha} c_{\boldsymbol{k}\alpha} - \Delta\, c^\dagger_{\boldsymbol{k}\alpha} \sigma^z_{\alpha\alpha} c_{\boldsymbol{k}+\boldsymbol{K},\alpha} \right] + \text{constant}. \tag{50}$$

The is the analog of the BCS Hamiltonian for superconductivity, and the analog of the pairing gap is the energy

$$\Delta = \lambda \mathcal{N}\,. \tag{51}$$

But, in general, the spectrum of $H_{\rm AFM}$ does not have a gap, as we will see below. As in BCS theory, the value of $\mathcal{N}$ has to be determined self-consistently from the mean-field equations.

To obtain the fermionic excitation spectrum, we have to perform the analog of the Bogoliubov rotation in BCS theory. This is achieved by writing $H_{\rm AFM}$ in a 2×2 matrix form by using the fact that $2\boldsymbol{K}$ is a reciprocal lattice vector, and so $\varepsilon_{\boldsymbol{k}+2\boldsymbol{K}} = \varepsilon_{\boldsymbol{k}}$; correspondingly, the prime over the summation indicates that it only extends over half the Brillouin zone of the underlying lattice, shown in the left panel of Fig. 8, which is the Brillouin zone of the lattice with Néel order.

$$H_{\rm AFM} = {\sum_{\boldsymbol{k}}}' (c^\dagger_{\boldsymbol{k}\alpha}, c^\dagger_{\boldsymbol{k}+\boldsymbol{K},\alpha}) \begin{pmatrix} \varepsilon_{\boldsymbol{k}} & -\Delta\sigma^z_{\alpha\alpha} \\ -\Delta\sigma^z_{\alpha\alpha} & \varepsilon_{\boldsymbol{k}+\boldsymbol{K}} \end{pmatrix} \begin{pmatrix} c_{\boldsymbol{k}\alpha} \\ c_{\boldsymbol{k}+\boldsymbol{K},\alpha} \end{pmatrix}. \tag{52}$$

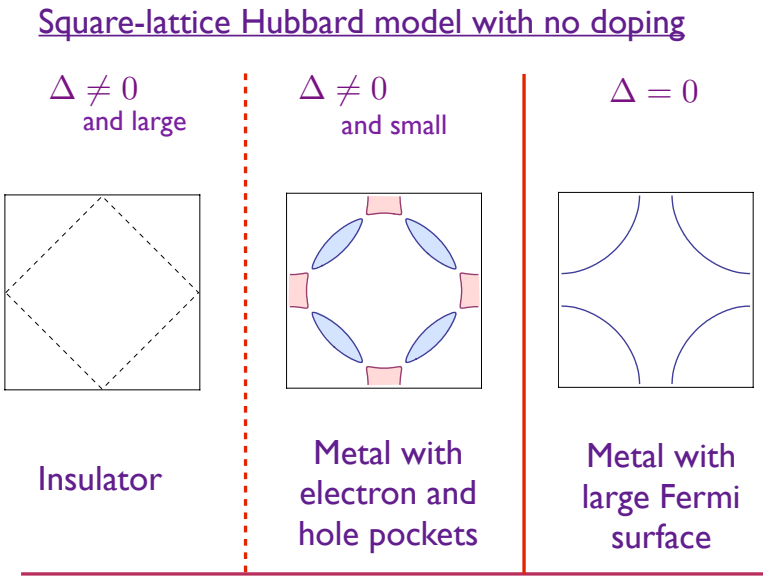

FIG. 8. Fermi surfaces of the Néel state at doping $p = 0$. The pockets intersecting the diagonals of the Brillouin zone have both bands in (53) empty and so form hole pockets, while the remaining pockets have both bands occupied and form electron pockets. The dashed line in the insulator shows the boundary of the Brillouin zone of the Néel state

It is now easy to diagonalize the 2×2 matrix in (52), and we obtain

$$E_{\boldsymbol{k}\pm} = \frac{\varepsilon_{\boldsymbol{k}} + \varepsilon_{\boldsymbol{k}+\boldsymbol{K}}}{2} \pm \left[\left(\frac{\varepsilon_{\boldsymbol{k}} - \varepsilon_{\boldsymbol{k}+\boldsymbol{K}}}{2} \right)^2 + \Delta^2 \right]^{1/2} \tag{53}$$

Unlike the BCS spectrum, the spectrum in (53) is not gapped, or even positive definite. Rather, it is the spectrum of a metal, in which the negative energy states are filled, and bounded by a Fermi surface. The Fermi surfaces so obtained is shown in Figs. 8, 9, 10 for different values of p.

We observe that the 'large' Fermi surface of the paramagnetic metal has 'reconstructed' into small pocket Fermi surfaces in the SDW state. The excitations of the SDW metal are hole-like quasiparticles on the Fermi surfaces surrounding the hole pockets, and electron-like quasiparticles on the Fermi surfaces surrounding the electron pockets. The spin wave excitations interact rather weakly with the fermionic quasiparticle excitations: this can be see from a somewhat involved computation from the effective action.

Finally we discuss the fate of the Luttinger relation of Section I D in this metal. The Luttinger relation connects the volume enclosed by the Fermi surface to the density of electrons, modulo 2 electrons per unit cell. It should be applied in the Brillouin zone of the Néel state, which is half the size of the Brillouin zone of the underlying square lattice, as shown in Fig. 8. In real space, this corresponds to the fact that the unit cell has doubled, and so the density of electrons per unit

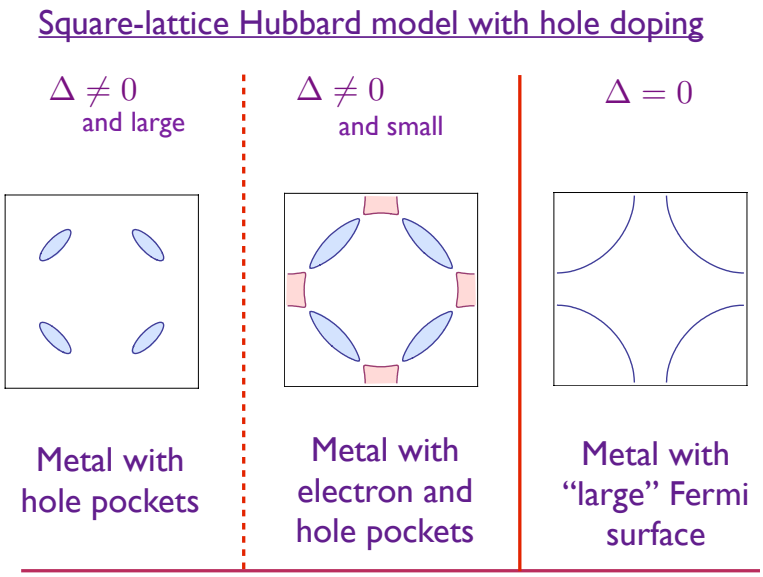

FIG. 9. Fermi surfaces of the Néel state at $p > 0$. The pockets are as in Fig. 8.

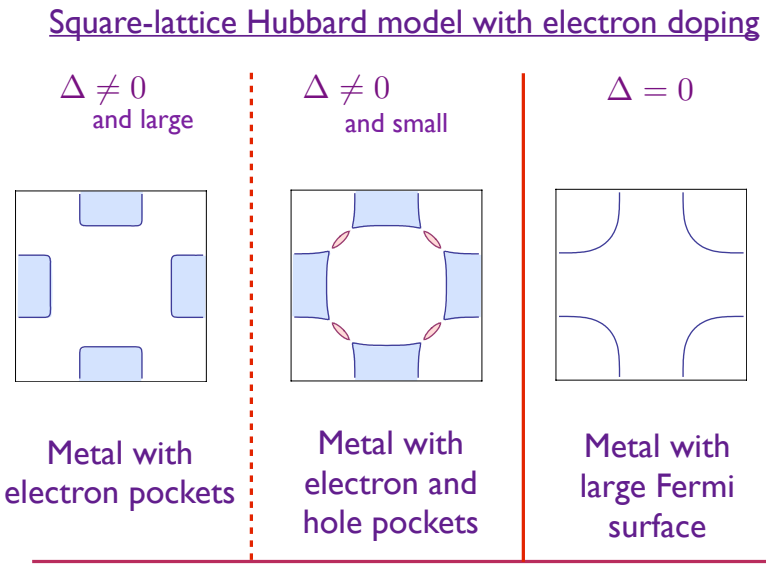

FIG. 10. Fermi surfaces of the Néel state at $p < 0$, with pockets as in Figs. 8.

cell is $2(1-p)$. For spinful electrons, the Luttinger relations measures electron density modulo 2, and so the density appearing in the Luttinger relation is $-2p$. This has to be equated to twice the volumes enclosed by the electron and hole pockets within the diamond shaped Brillouin zone in Fig. 8. Let $\mathcal{A}_h$ be the area of a single elliptical hole pocket: there are 4 such pockets in the complete Brillouin zone of the square lattice or 2 pockets in the Brillouiin zone of the Néel state,

as is apparent from Figs. 8, 9, 10. Similarly, let $\mathcal{A}_e$ be the area of a single elliptical electron pocket: there are 2 such pockets in the complete Brillouin zone of the square lattice or 1 pocket in the Brillouin zone of the Néel state. These arguments show that the Luttinger relation becomes

$$2 \times \frac{1}{(2\pi)^2/2} \times (-2\mathcal{A}_h + \mathcal{A}_e) = -2p\,. \tag{54}$$

On the left hand side, the first factor is the spin degeneracy, and the second factor is the inverse of the volume of the Brillouin zone of the Néel state. To reiterate, this is the conventional Luttinger relation applied after accounting for the doubling of the unit cell, and it determines a linear constraint on the areas of the electron and hole pockets.

V. FERMI VOLUME CHANGE IN A METAL

See slides at https://sachdev.physics.harvard.edu/UQM24FLs.pdf.

VI. THE SYK MODEL

See slides at https://sachdev.physics.harvard.edu/UQM24SYK.pdf.

The Hamiltonian of a version of a SYK model is illustrated in Fig. 11. A system with fermions c_i, $i = 1 \ldots N$ states is assumed. Depending upon physical realizations, the label i could be position or an orbital, and it is best to just think of it as an abstract label of a fermionic qubit with the two states $|0\rangle$ and $c_i^\dagger |0\rangle$. $\mathcal{Q}N$ fermions are placed in these states, so that a density $\mathcal{Q} \approx 1/2$ is occupied, as shown in Fig. 11. The quantum dynamics is restricted to *only* have a 'collision' term between the fermions, analogous to the right-hand-side of the Boltzmann equation. However, in stark contrast to the Boltzmann equation, statistically independent collisions are not assumed, and quantum interference between successive collisions is accounted for: this is the key to building up a many-body state with non-trivial entanglement. So a collision in which fermions move from sites i and j to sites k and ℓ is characterized not by a probability, but by a quantum amplitude $U_{ij;k\ell}$, which is a complex number.

The model so defined has a Hilbert space of order 2^N states, and a Hamiltonian determined by order N^4 numbers $U_{ij;k\ell}$. Determining the spectrum or dynamics of such a Hamiltonian for large N seems like an impossibly formidable task. But with the assumption that the $U_{ij;k\ell}$ are statistically independent random numbers, remarkable progress is possible. Note that an ensemble of SYK models with different $U_{ij;k\ell}$ is not being considered, but a single fixed set of $U_{ij;k\ell}$. Most physical properties of this model are self-averaging at large N, and so as a technical tool, they can be rapidly obtained by computations on an ensemble of random $U_{ij;k\ell}$. In any case, the analytic results described below have been checked by numerical computations on a computer for a fixed

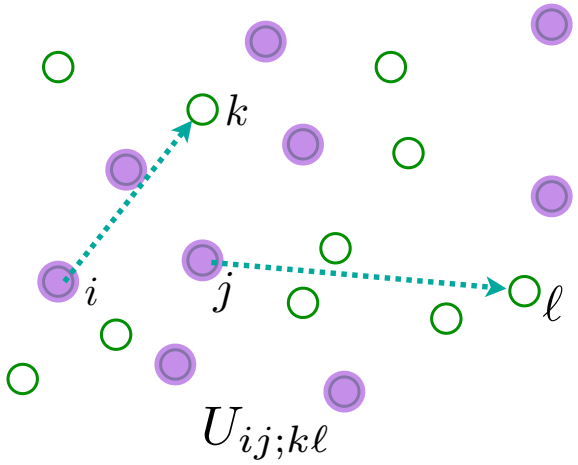

FIG. 11. The SYK model: fermions undergo the transition ('collision') shown with quantum amplitude $U_{ij;k\ell}$.

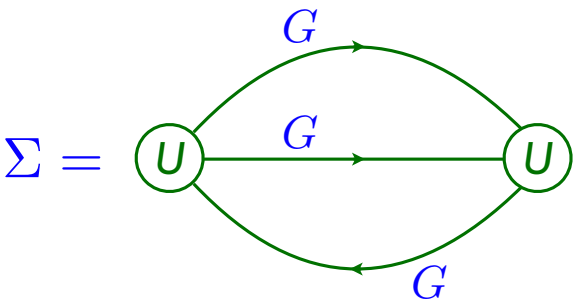

FIG. 12. Self-energy for the fermions of $\mathcal{H}$ in (55) in the limit of large N. The intermediate Green's functions are fully renormalized.

set of $U_{ij;k\ell}$. Recall that, even for the Boltzmann equation, there was an ensemble average over the initial positions and momenta of the molecules that was implicitly performed.

Specifically, the Hamiltonian in a chemical potential μ is

$$\mathcal{H} = \frac{1}{(2N)^{3/2}} \sum_{i,j,k,\ell=1}^{N} U_{ij;k\ell}\, c_i^\dagger c_j^\dagger c_k c_\ell - \mu \sum_i c_i^\dagger c_i \tag{55}$$

$$c_i c_j + c_j c_i = 0 \quad , \quad c_i c_j^\dagger + c_j^\dagger c_i = \delta_{ij} \tag{56}$$

$$\mathcal{Q} = \frac{1}{N} \sum_i c_i^\dagger c_i \,; \quad [\mathcal{H}, \mathcal{Q}] = 0 \,; \quad 0 \le \mathcal{Q} \le 1 \,, \tag{57}$$

and its large N limit is most simply taken graphically, order-by-order in $U_{ij;k\ell}$, and averaging over $U_{ij;k\ell}$ as independent random variables with $\overline{U_{ij;k\ell}} = 0$ and $\overline{|U_{ij;k\ell}|^2} = U^2$. This expansion can be

used to compute graphically the Green's function in imaginary time τ

$$G(\tau) = -\frac{1}{N}\sum_i \overline{\left\langle \mathcal{T}\left(c_i(\tau)c_i^\dagger(0)\right)\right\rangle}\,, \tag{58}$$

where $\mathcal{T}$ is the time-ordering symbol, the angular brackets are a quantum average for any given $U_{ij;k\ell}$, and the over-line denotes an average over the ensemble of $U_{ij;k\ell}$. (It turns out that the last average is not needed for large N, because the quantum observable is self-averaging.) In the large N limit, only the graph for the Dyson self energy, Σ, in Fig. 12 survives, and the on-site fermion Green's function is given by the solution of the following equations

$$\begin{aligned} G(i\omega_n) &= \frac{1}{i\omega_n + \mu - \Sigma(i\omega_n)} \\ \Sigma(\tau) &= -U^2 G^2(\tau) G(-\tau) \\ G(\tau = 0^-) &= \mathcal{Q}\,, \end{aligned} \tag{59}$$

where ω_n is a fermionic Matsubara frequency. The first equation in (59) is the usual Dyson relation between the Green's function and self energy in quantum field theory, the second equation in (59) is the Feynman graph in Fig. 12, and the last determines the chemical potential μ from the charge density $\mathcal{Q}$. These equations can also be obtained as saddle-point equations of the following exact representation of the disordered-averaged partition function, expressed as a '$G-\Sigma$' theory [5–8]:

$$\begin{aligned} \mathcal{Z} &= \int \mathcal{D}G(\tau_1,\tau_2)\mathcal{D}\Sigma(\tau_1,\tau_2)\exp(-NI) \\ I &= \ln\det\left[\delta(\tau_1-\tau_2)(\partial_{\tau_1}+\mu) - \Sigma(\tau_1,\tau_2)\right] \\ &\quad + \int d\tau_1 d\tau_2 \left[\Sigma(\tau_1,\tau_2)G(\tau_2,\tau_1) + (U^2/2)G^2(\tau_2,\tau_1)G^2(\tau_1,\tau_2)\right] \end{aligned} \tag{60}$$

This is a path-integral over bi-local in time functions $G(\tau_1,\tau_2)$ and $\Sigma(\tau_1,\tau_2)$, whose saddle point values are the Green's function $G(\tau_1-\tau_2)$, and the self energy $\Sigma(\tau_1-\tau_2)$. This bi-local G can be viewed as a composite quantum operator corresponding to an on-site fermion bilinear

$$G(\tau_1,\tau_2) = -\frac{1}{N}\sum_i \mathcal{T}\left(c_i(\tau_1)c_i^\dagger(\tau_2)\right) \tag{61}$$

that is averaged in (58).

For general ω and T, the equations in (59) have to be solved numerically. But an exact analytic solution is possible in the limit $\omega, T \ll U$. At $T=0$, the asymptotic forms can be obtained straightforwardly [9]

$$G(i\omega) \sim -i\mathrm{sgn}(\omega)|\omega|^{-1/2} \quad , \quad \Sigma(i\omega) - \Sigma(0) \sim -i\mathrm{sgn}(\omega)|\omega|^{1/2}\,, \tag{62}$$

and a more complete analysis of (59) gives the exact form at non-zero T ($\hbar = k_B = 1$) [10]

$$G(\omega) = \frac{-iCe^{-i\theta}}{(2\pi T)^{1/2}} \frac{\Gamma\left(\frac{1}{4} - \frac{i\omega}{2\pi T} + i\mathcal{E}\right)}{\Gamma\left(\frac{3}{4} - \frac{i\omega}{2\pi T} + i\mathcal{E}\right)} \qquad |\omega|, T \ll U\,. \tag{63}$$

Here, $\mathcal{E}$ is a dimensionless number which characterizes the particle-hole asymmetry of the spectral function; both $\mathcal{E}$ and the pre-factor C are determined by an angle $-\pi/4 < \theta < \pi/4$

$$e^{2\pi\mathcal{E}} = \frac{\sin(\pi/4+\theta)}{\sin(\pi/4-\theta)} \quad , \quad C = \left(\frac{\pi}{U^2\cos(2\theta)}\right)^{1/4} , \tag{64}$$

and the value of θ is determined by a Luttinger relation to the density $\mathcal{Q}$ [5]

$$\mathcal{Q} = \frac{1}{2} - \frac{\theta}{\pi} - \frac{\sin(2\theta)}{4}\,. \tag{65}$$

A notable property of (63) at $\mathcal{E} = 0$ is that it equals the temporal Fourier transform of the spatially local correlator of a fermionic field of dimension 1/4 in a conformal field theory in 1+1 spacetime dimensions. A theory in 0+1 dimensions is considered here, where conformal transformations map the temporal circle onto itself, as reviewed in Appendices A and B of Ref. [11]; such transformations allow a non-zero $\mathcal{E}$. An important consequence of this conformal invariance is that (63) is a scaling function of $\hbar\omega/(k_B T)$ (after restoring fundamental constants); in other words, the characteristic frequency scale of (63) is determined solely by $k_B T/\hbar$, is independent of the value of $U/\hbar$. A careful study of the consequences of this conformal invariance have established the following properties of the SYK model (more complete references to the literature are given in other reviews [11, 12]):

- There are no quasiparticle excitations, and the SYK model exhibits quantum dynamics with a 'Planckian' relaxation time of order $\hbar/(k_B T)$ at $T \ll U$. In particular, the relaxation time is *independent* of U, a feature not present in any ordinary metal with quasiparticles. While the Planckian relaxation in (63) implies the absence of quasiparticles with the same quantum numbers as the c fermion, it does not rule out the possibility that c has fractionalized into some emergent quasiparticles; this possibility is ruled out by the exponentially large number of low energy states, as discussed below.

- At large N, the many-body density of states at fixed $\mathcal{Q}$ is [7, 8, 13–16] (see Fig. 13a)

$$D(E) \sim \frac{1}{N}\exp(N s_0)\sinh\left(\sqrt{2N\gamma E}\right)\,, \tag{66}$$

  where the ground state energy has been set to zero. Here s_0 is a universal number dependent only on $\mathcal{Q}$ ($s_0 = 0.4648476991708051\ldots$ for $\mathcal{Q} = 1/2$), $\gamma \sim 1/U$ is the only parameter

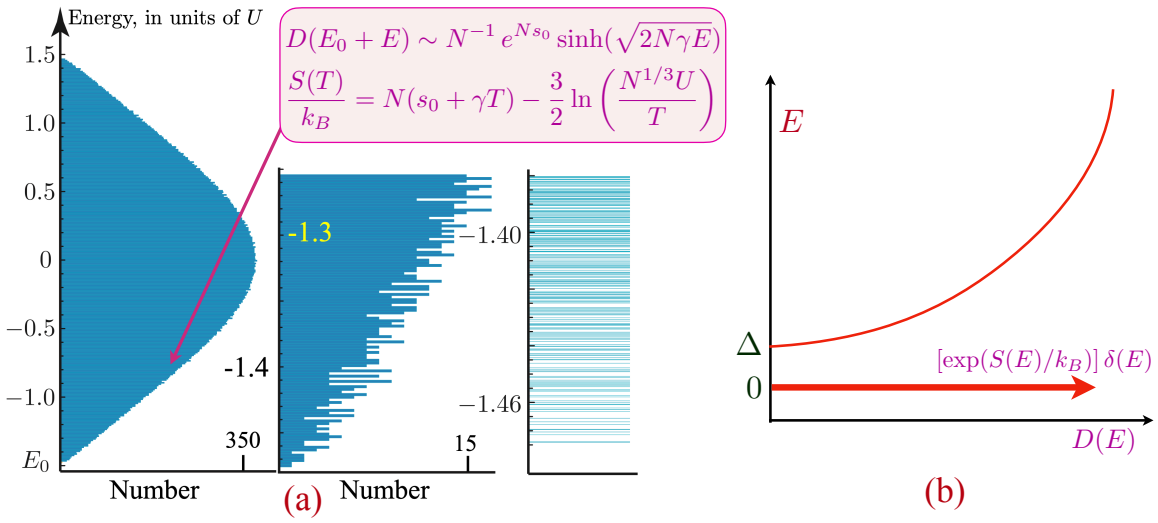

FIG. 13. (a) Plot of the 65536 many-body eigenvalues of a $N = 32$ Majorana SYK Hamiltonian; however, the analytical results quoted here are for the SYK model with complex fermions which has a similar spectrum. The coarse-grained low-energy and low-temperature behavior is described by (66) and (68). (b) Schematic of the lower energy density of states of a supersymmetric generalization of the SYK model [15, 17]. There is a delta function at $E = 0$, and the energy gap Δ is proportional to the inverse of $S(E = 0)$.

dependent upon the strength of the interactions, and the N dependence of the pre-factor is discussed in Ref. [16]. Given $D(E)$, the partition function can be computed from

$$\mathcal{Z} = \int_{0^-}^{\infty} dE D(E) \exp\left(-\frac{E}{k_B T}\right) . \tag{67}$$

at a temperature T, and hence the low-T dependence of the entropy at fixed Q is given by

$$\frac{S(T)}{k_B} = N(s_0 + \gamma\, k_B T) - \frac{3}{2}\ln\left(\frac{U}{k_B T}\right) - \frac{\ln N}{2} + \ldots . \tag{68}$$

The thermodynamic limit $\lim_{N\to\infty} S(T)/N$ yields the microcanonical entropy

$$S(E)/k_B = Ns_0 + \sqrt{2N\gamma E}\,, \tag{69}$$

and this connects to the extensive E limit of (66) after using Boltzmann's formula. The limit $\lim_{T\to 0}\lim_{N\to\infty} S(T)/(k_B N) = s_0$ is non-zero, implying an energy-level spacing exponentially small in N near the ground state: the density of states (66) implies that any small energy interval near the ground state contains an exponentially large number of energy eigenstates (see Fig. 13a). This is very different from systems with quasiparticle excitations, whose energy level spacing vanishes with a positive power of $1/N$ near the ground state,

as quasiparticles have order N quantum numbers. The exponentially small level spacing therefore rules out the existence of quasiparticles in the SYK model.

- However, it important to note that there is no exponentially large degeneracy of the ground state itself in the SYK model, unlike that in a supersymmetric generalization of the SYK model (see Fig. 13b) and the ground states in Pauling's model of ice [18]. Obtaining the ground-state degeneracy requires the opposite order of limits between T and N, and numerical studies show that the entropy density does vanish in such a limit for the SYK model. The many-particle wavefunctions of the low-energy eigenstates in Fock space change chaotically from one state to the next, providing a realization of maximal many-body quantum chaos [19] in a precise sense. This structure of eigenstates is very different from systems with quasiparticles, for which the lowest energy eigenstates differ only by adding and removing a few quasiparticles.

- The E dependence of the density of states in (66) is associated with a time reparameterization mode, and (66) shows that its effects are important when $E \sim 1/N$. The low energy quantum fluctuations of (60) can be expressed in terms of a path integral which reparameterizes imaginary time $\tau \to f(\tau)$, in a manner analogous to the quantum theory of gravity being expressed in terms of the fluctuations of the spacetime metric. There are also quantum fluctuations of a phase mode $\phi(\tau)$, whose time derivative is the charge density, and the path integral in (60) reduces to the partition function

$$\mathcal{Z}_{SYK-TR} = e^{N s_0} \int \mathcal{D}f \mathcal{D}\phi \exp\left(-\frac{1}{\hbar} \int_0^{\hbar/(k_B T)} d\tau \, \mathcal{L}_{SYK-TR}[f,\phi] \right) \tag{70}$$

  The Lagrangian $\mathcal{L}_{SYK-TR}$ is known, and involves a Schwarzian of $f(\tau)$. Remarkably, despite its non-quadratic Lagrangian, the path integral in (70) can be performed exactly [15], and leads to (66).

A. The Yukawa-SYK model

The SYK model defined above is a 0+1 dimensional theory with no spatial structure, and so cannot be directly applied to transport of strange metals in non-zero spatial dimensions. A great deal of work has been undertaken on generalizing the SYK model to non-zero spatial dimensions [11], but this effort has ultimately not been successful: although 'bad metal' states have been obtained, low T strange metals have not. But another effort based upon a variation of the SYK model, the 0+1 dimensional 'Yukawa-SYK' model [17, 20–30], has been a much better starting point for a non-zero spatial dimensional theory, as shown in Section VIII. The present subsection describes the basic properties of the simplest realization [24, 28–30] of the Yukawa-SYK model.

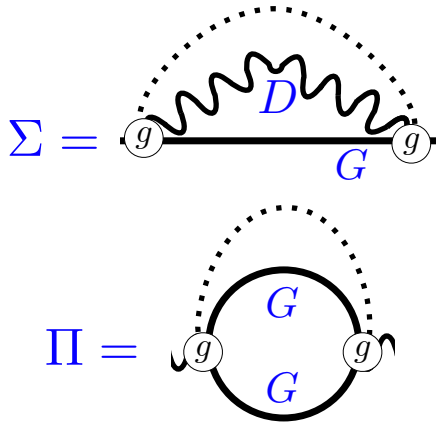

FIG. 14. Self-energies of the fermions and bosons in the Hamiltonian $\mathcal{H}_Y$ in (71). The intermediate Green's functions are fully renormalized.

In the spirit of (55), a model of fermions c_i ($i = 1 \dots N$) and bosons ϕ_ℓ ($\ell = 1 \dots N$) with a Yukawa coupling $g_{ij\ell}$ between them is now considered

$$\mathcal{H}_Y = -\mu \sum_i c_i^\dagger c_i + \sum_\ell \frac{1}{2}\left(\pi_\ell^2 + \omega_0^2 \phi_\ell^2\right) + \frac{1}{N}\sum_{ij\ell} g_{ij\ell} c_i^\dagger c_j \phi_\ell \,, \tag{71}$$

with $g_{ij\ell}$ independent random numbers with zero mean and r.m.s. value g. The bosons are oscillators with the same frequency ω_0, while the fermions have no one-particle hopping. The large N limit of (71) can be taken just as for the SYK model in (55). The self-energy graph in Fig. 12 is replaced by those in Fig. 14: the phonon Green's function is D, while the phonon self-energy is Π.

Continuing the parallel with the SYK model, the disorder-averaged partition function of the Yukawa-SYK model is a bi-local G-Σ-D-Π theory, analogous to (60):

$$\begin{aligned} \mathcal{Z} &= \int \mathcal{D}G\, \mathcal{D}\Sigma\, \mathcal{D}D\, \mathcal{D}\Pi \exp(-N S_{\rm all}) \\ S_{\rm all} &= -\ln\det(\partial_\tau - \mu + \Sigma) + \frac{1}{2}\ln\det(-\partial_\tau^2 + \omega_0^2 - \Pi) \\ &\quad + \int d\tau \int d\tau' \left[-\Sigma(\tau';\tau) G(\tau,\tau') + \frac{1}{2}\Pi(\tau',\tau) D(\tau,\tau') + \frac{g^2}{2} G(\tau,\tau') G(\tau',\tau) D(\tau,\tau') \right] . \end{aligned} \tag{72}$$

The large N saddle-point equations replacing (59) are:

$$\begin{aligned} G(i\omega_n) = \frac{1}{i\omega_n + \mu - \Sigma(i\omega_n)} \quad &, \quad D(i\omega_n) = \frac{1}{\omega_n^2 + \omega_0^2 - \Pi(i\omega_n)} \\ \Sigma(\tau) = g^2 G(\tau) D(\tau) \quad &, \quad \Pi(\tau) = -g^2 G(\tau) G(-\tau) \end{aligned} \tag{73}$$

The solution of (72) and (73) leads to a critical state with properties very similar to that of the SYK model [24, 28–30]. Only the low-frequency behavior of the Green's functions at $T = 0$, is

quoted analogous to (62):

$$G(i\omega) \sim -i\mathrm{sgn}(\omega)|\omega|^{-(1-2\Delta)} \quad , \quad D(i\omega) \sim |\omega|^{1-4\Delta} \quad , \quad \frac{1}{4} < \Delta < \frac{1}{2} \, . \tag{74}$$

Inserting the ansatz (74) into (73) fixes the value of the critical exponent Δ.

$$\frac{4\Delta - 1}{2(2\Delta - 1)[\sec(2\pi\Delta) - 1]} = 1 \quad , \quad \Delta = 0.42037\ldots \tag{75}$$

Although the fermion Green's function has an exponent which differs from that of the SYK model, the thermodynamic properties have the same structure as that of the SYK model, including the presence of the Schwarzian mode and the form of the many-body density of states.

VII. QUANTUM CRITICALITY OF CLEAN METALS

See slides at https://sachdev.physics.harvard.edu/UQM24QCM.pdf.

Following the example of the Yukawa-SYK model in Section VI A, it was argued [31–33] that problems of fermions coupled to a critical boson could also be addressed by examining ensembles of theories with different Yukawa couplings. It is also possible to choose the ensemble so that the couplings are spatially independent, and this maintains full translational symmetry in each member of the ensemble. If most members of the ensemble flow to the same universal low energy theory, then we can access the low energy behavior by studying the average over the ensemble. We also obtain the added benefit of a G-Σ action with large N prefactor, which allows for a systematic treatment of the theory.

Here we consider the case of an order parameter of a broken symmetry at zero momentum, such as Ising ferromagnetism of Section III. Similar analyses apply to the cases in Sections IV and V, but will not be discussed here. So we consider the following generalization of the theory (39)

$$\begin{aligned} \mathcal{L} = \sum_{\alpha=1}^{N} \sum_{\boldsymbol{k}} c^{\dagger}_{\boldsymbol{k},\alpha} \left[\frac{\partial}{\partial \tau} + \varepsilon(\boldsymbol{k}) \right] c_{\boldsymbol{k},\alpha} + \int d^2 r \sum_{\gamma=1}^{M} \left\{ \frac{1}{2} \left[(\boldsymbol{\nabla} \phi_\gamma)^2 + (\partial_\tau \phi_\gamma)^2 + s \, \phi_\gamma^2 \right] \right\} \\ - \int d^2 r \sum_{\gamma=1}^{M} \sum_{\alpha,\beta=1}^{N} \frac{g_{\alpha\beta\gamma}}{N} \phi_\gamma \, c^{\dagger}_{\alpha} c_\beta \, . \end{aligned} \tag{76}$$

Here the fermion has N components, the boson has M components, and we take the large N limit with

$$\lambda = \frac{M}{N} \tag{77}$$

fixed. The Yukawa coupling is taken to be a random function of the flavor indices with

$$\overline{g_{\alpha\beta\gamma}} = 0 \, , \quad g^*_{\alpha\beta\gamma} = g_{\beta\alpha\gamma} \, , \quad \overline{|g_{\alpha\beta\gamma}|^2} = g^2 \, . \tag{78}$$

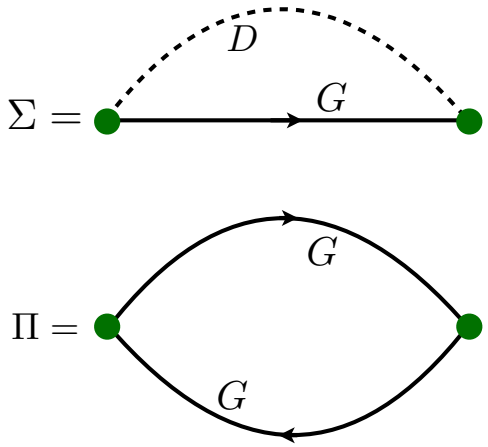

FIG. 15. Saddle point equations for the fermion self energy Σ and boson self energy Π, expressed in terms of the renormalized fermion Green's function G and boson Green's function D. The filled circle is the Yukawa coupling $g_{\alpha\beta\gamma}$.

We have dropped the quartic self-coupling u of the the scalar field for simplicity: it is unimportant for the leading critical behavior, but is needed for certain sub-leading effects at non-zero temperature [33]. The original theory in (39) has a $\phi \to -\phi$ symmetry which is only statistically present in (76): we can maintain this symmetry in each member of the ensemble by dividing the indices into groups of 2, but we avoid this complexity because it does not modify the large N results. We consider an ensemble of complex couplings because it simplifies the analysis, but real couplings lead to essentially the same results.

We can now proceed with the large N analysis following the script of the Yukawa-SYK model. As in Section VI A, the large N saddle point equations are most easily obtained by a diagrammatic perturbation theory in g, in which we average each graph order-by-order. In the large N limit, only the graphs shown in Fig. 15 survive, and yield the following saddle point equations

$$\begin{aligned}
\Sigma(\boldsymbol{r},\tau) &= g^2\lambda D(\boldsymbol{r},\tau)G(\boldsymbol{r},\tau),\\
\Pi(\boldsymbol{r},\tau) &= -g^2 G(-\boldsymbol{r},-\tau)G(\boldsymbol{r},\tau),\\
G(\boldsymbol{k},i\omega_n) &= \frac{1}{i\omega_n - \varepsilon(\boldsymbol{k}) - \Sigma(\boldsymbol{k},i\omega_n)},\\
D(\boldsymbol{q},i\Omega_m) &= \frac{1}{\Omega_m^2 + q^2 + s - \Pi(\boldsymbol{q},i\Omega_m)}.
\end{aligned} \tag{79}$$

Here G is the Green's function for the fermion c, and Σ its self energy, and D is the Green's function for the boson f, and Π is its self energy.

The equations (79) are the analog of the Yukawa-SYK equations in (73), but the Green's functions now involve both spatial and temporal arguments. Remarkably, as we shall see in Section VII A, an exact solution of the low energy scaling behavior is possible for (79), just as

it was for the Yukawa-SYK model.

For completeness, we also write down the path integral of the averaged theory using bilocal Green's functions, the analog of (60) for the SYK model. We introduce the spacetime co-ordinate $X \equiv (\tau, x, y)$, and all Green's functions and self energies in the path integral are functions of two spacetime co-ordinates X_1 and X_2. Then we have

$$\begin{aligned}\overline{\mathcal{Z}} = \int \mathcal{D}G(X_1, X_2)\mathcal{D}\Sigma(X_1, X_2)\mathcal{D}D(X_1, X_2) \\ \times \mathcal{D}\Pi(X_1, X_2) \exp\left[-NI(G, \Sigma, D, \Pi)\right] .\end{aligned} \tag{80}$$

The G-Σ-D-Π action is now

$$\begin{aligned}I(G, \Sigma, D, \Pi) = \frac{g^2\lambda}{2}\mathrm{Tr}\left(G \cdot [GD]\right) - \mathrm{Tr}(G \cdot \Sigma) + \frac{\lambda}{2}\mathrm{Tr}(D \cdot \Pi) \\ - \ln\det\left[\left(\partial_{\tau_1} + \varepsilon(-i\boldsymbol{\nabla}_1)\right)\delta(X_1 - X_2) + \Sigma(X_1, X_2)\right] \\ + \frac{\lambda}{2}\ln\det\left[\left(-\partial_{\tau_1}^2 - \boldsymbol{\nabla}_1^2 + s\right)\delta(X_1 - X_2) - \Pi(X_1, X_2)\right] .\end{aligned} \tag{81}$$

where we have introduced notation

$$\mathrm{Tr}\left(f \cdot g\right) \equiv \int dX_1 dX_2\, f(X_2, X_1) g(X_1, X_2) . \tag{82}$$

Note the crucial pre-factor of N before I in the path-integral. It can be verified that the saddle point equations of (81) reduce to (79).

A. Patch solution

This subsection will present an exact solution of the saddle point equations (79) in the low energy scaling limit. We will be able to obtain this solution for an arbitrary $\varepsilon(\boldsymbol{k})$, and for a general shape of the Fermi surface. The key to the solution is the observation that the singular behavior at any point on the Fermi surface is determined only by a small momentum space patch around it, as well as that of the anti-podal point. We do need to include the curvature of the Fermi surface though, and it is not sufficient to think of the Fermi surface as a set of one-dimensional chiral fermions at each point on the Fermi surface.

We begin by evaluating Π in (79) using the bare fermion Green's function. This yields the Lindhard susceptibility in (46) and (47)

$$\begin{aligned}\Pi(\boldsymbol{q}, i\Omega_m) &= -g^2 T \sum_{\omega_n} \int \frac{d^2k}{4\pi^2} \frac{1}{(i(\omega_n + \Omega_m) - \varepsilon(\boldsymbol{k} + \boldsymbol{q}))(i\omega_n - \varepsilon(\boldsymbol{k}))} \\ &= g^2 \int \frac{d^2k}{4\pi^2} \frac{f(\varepsilon(\boldsymbol{k} + \boldsymbol{q})) - f(\varepsilon(\boldsymbol{k}))}{i\Omega_m + \varepsilon(\boldsymbol{k}) - \varepsilon(\boldsymbol{k} + \boldsymbol{q})} ,\end{aligned} \tag{83}$$

where $f(\varepsilon)$ is the Fermi function. We are interested in the behavior of Π for small $\boldsymbol{q}$ and Ω_m at low T. On the real frequency axis, the real part of Π is not universal , and depends in a complicated

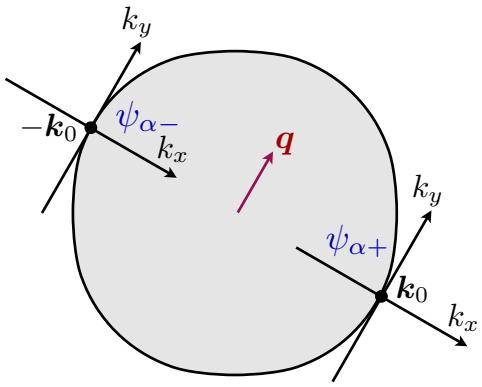

FIG. 16. Points $\pm\boldsymbol{k}_0$ on the Fermi surface which satisfy (85). The momentum of the boson is $\boldsymbol{q}$, and the low energy fermion contributions arise from momenta in the vicinity of $\pm\boldsymbol{k}$.

manner on the entire fermion dispersion. However, the behavior of the imaginary part of Π is much simpler and universal. We have

$$\begin{aligned}\mathrm{Im}\,\Pi(\boldsymbol{q},\Omega) &= -\pi g^2 \int \frac{d^2k}{4\pi^2}\,\left[f(\varepsilon(\boldsymbol{k}+\boldsymbol{q}))-f(\varepsilon(\boldsymbol{k}))\right]\delta\left(\Omega+\varepsilon(\boldsymbol{k})-\varepsilon(\boldsymbol{k}+\boldsymbol{q})\right)\\ &= \pi g^2\Omega\int \frac{d^2k}{4\pi^2}\,\delta\left(\varepsilon(\boldsymbol{k})\right)\delta\left(\Omega+\varepsilon(\boldsymbol{k})-\varepsilon(\boldsymbol{k}+\boldsymbol{q})\right)\quad \text{as } T\to 0. \end{aligned} \tag{84}$$

The last expression contains an integral over 2-dimensional momentum space of $\boldsymbol{k}$, along with 2 delta functions containing arguments which are functions of $\boldsymbol{k}$. Generically, both delta functions will be satisfied only at isolated points in momentum space. For $|\boldsymbol{q}|, |\Omega| \to 0$, the isolated points are solutions of

$$\varepsilon(\boldsymbol{k}) = 0 \quad \text{and} \quad \boldsymbol{q}\cdot\boldsymbol{\nabla}_{\boldsymbol{k}}\varepsilon(\boldsymbol{k}) = 0\,. \tag{85}$$

The solution of (85) is illustrated in Fig. 16: for a simply connected, convex Fermi surface, each direction of $\boldsymbol{q}$ is identified with the 2 anti-podal points $\pm\boldsymbol{k}_0$ on the Fermi surface where $\boldsymbol{q}$ is parallel to the tangent to the Fermi surface. Note that the value of $\boldsymbol{k}_0$ is fully determined by $\boldsymbol{q}$, but we leave this dependence implicit.

As illustrated in Fig. 16, we choose our momentum space axes so that $\boldsymbol{q} = (0, q_y)$. In the vicinity of $\boldsymbol{k}_0$ we write the fermion dispersion near the Fermi surface patch at $\boldsymbol{k}_0$ as

$$\boldsymbol{k} = \boldsymbol{k}_0 + (k_x, k_y), \quad \varepsilon(\boldsymbol{k}) = v_F k_x + \frac{\kappa}{2}k_y^2\,, \tag{86}$$

whereas near $-\boldsymbol{k}_0$ we have

$$\boldsymbol{k} = -\boldsymbol{k}_0 + (k_x, k_y), \quad \varepsilon(\boldsymbol{k}) = -v_F k_x + \frac{\kappa}{2}k_y^2\,. \tag{87}$$

Here v_F is the Fermi velocity, and κ is the curvature of the Fermi surface. The values of v_F and κ depend upon $\boldsymbol{k}_0$ which in turn depends upon $\boldsymbol{q}$, and they will vary as $\boldsymbol{k}_0$ moves around the Fermi

surface, but we have not explicitly indicated that; our results will remain valid even in the presence of such variation. We can now insert (86) into (84) and obtain the Landau damping result

$$\begin{aligned}\mathrm{Im}\,\Pi(\boldsymbol{q},\Omega) &= 2\pi g^2\Omega\int\frac{d^2k}{4\pi^2}\,\delta\left(v_F k_x+\kappa k_y^2/2\right)\delta\left(\kappa k_y q_y+q_y^2/2-\Omega\right)\\ &= \frac{g^2\Omega}{2\pi v_F\kappa|q_y|}\end{aligned} \tag{88}$$

where the leading factor of 2 is from the sum over the anti-podal points. Note that the curvature κ appears in the denominator, and so it is not valid to take the $\kappa\to 0$ limit, and no description in terms of purely linearly-dispersing excitations around the Fermi surface is possible.

Let us now turn to an evaluation of Π in (79) using the fully renormalized Green's function. Remarkably, as we will now show, the result in (88) remains largely unchanged. We anticipate that full solution of (79) leads to a fermion Green's function of the following form

$$\Sigma(\boldsymbol{k},i\omega_n)=\Sigma_0(\boldsymbol{k})+\Sigma(i\omega_n) \tag{89}$$

The momentum dependence of $\Sigma_0(\boldsymbol{k})$ will be non-singular, and we assume it can be absorbed by redefinition of the values of v_F and κ; we will therefore not include it in the computations below. The frequency dependent part $\Sigma(i\omega_n)$ can be singular (as we will see below) but it has no dependence on k_x and k_y; however it will depend upon the choice of $\boldsymbol{k}_0$, via the implicit $\boldsymbol{k}_0$ dependence of v_F and κ. We now insert $\Sigma(i\omega_n)$ into the first expression in (83) and use the dispersion (86) to obtain

$$\begin{aligned}\Pi(\boldsymbol{q},i\Omega_m) = -2g^2T\sum_{\omega_n}\int\frac{d^2k}{4\pi^2}\,&\frac{1}{(i\omega_n-v_Fk_x-\kappa q_y^2/2-\Sigma(i\omega_n))}\\ \times\,&\frac{1}{(i(\omega_n+\Omega_m)-v_Fk_x-\kappa(k_y+q_y)^2/2-\Sigma(i\omega_n+i\Omega_m))}\,.\end{aligned} \tag{90}$$

At this point in (83) we evaluated the summation over the frequency ω_n, but we are unable to do that here because of the unknown frequency dependence in $\Sigma(i\omega_n)$. So we have instead decided to focus only on the contribution of the patches near $\pm\boldsymbol{k}_0$, and linearized the fermion dispersion accordingly. In this situation the dependence of the integrand on k_x and k_y is simple. Performing the integral over k_x in (90) we obtain

$$\begin{aligned}\Pi(\boldsymbol{q},i\Omega_m) = \frac{-ig^2T}{v_F}\sum_{\omega_n}\int\frac{dk_y}{(2\pi)}\,&[\mathrm{sgn}(\omega_n+\Omega_m)-\mathrm{sgn}(\omega_n)]\\ \times\,&\frac{1}{i\Omega_m-\kappa q_y^2/2-\kappa q_yk_y+\Sigma(i\omega_n)-\Sigma(i\omega_n+i\Omega_m)}\,.\end{aligned} \tag{91}$$

We have assumed here that $\mathrm{sgn}(\omega_n-\Sigma(i\omega_n)/i)=\mathrm{sgn}(\omega_n)$, and this always turn out to be the case from the positivity requirements of the fermion spectral weight. The next step is the evaluation of the q_y integral in (91). The real part of this integral is logarithmically divergent at large q_y, but

then we are no longer in a regime where it is valid to keep the linearized dispersion. We assume that the divergent pieces only yield non-singular contribution, and keep the singular imaginary part of the integral. In this manner, we obtain from (91)

$$\begin{aligned}\Pi(\boldsymbol{q}, i\Omega_m) &= \frac{g^2 T}{2\kappa v_F |q_y|} \sum_{\omega_n} \mathrm{sgn}(\Omega_m) \left[\mathrm{sgn}(\omega_n + \Omega_m) - \mathrm{sgn}(\omega_n)\right] \\ &= -\frac{g^2 |\Omega_m|}{2\pi\kappa v_F |q_y|} \,. \end{aligned} \tag{92}$$

This agrees precisely with (88), and all dependence on Σ has dropped out, as we claimed.

The final step in the exact solution of (79) is the evaluation of $\Sigma(i\omega_n)$ at the point $\boldsymbol{k}_0$ on the Fermi surface. As we noted earlier, the parameters v_F and κ depend smoothly upon the choice of $\boldsymbol{k}_0$, and this will be the only momentum dependence in the singular part of the fermion self energy. A careful evaluation first proceeds by the real frequency method used for Π in (84), and we can follow that method for the imaginary part of the $\Sigma(\omega)$ on the real frequency axis. Such an evaluation shows that the result is dominated by the fermions in the vicinity of $\boldsymbol{k}_0$, and with boson momentum $q_y \gg q_x$ which is nearly tangent to the Fermi surface. However, we proceed directly to the second method used for Π below (90) in which we integrate over momenta before we integrate over frequency: this has the advantage of allowing use to include $\Sigma(i\omega_n)$ in the fermion propagator. From the first equation in (79), using the linearized dispersion and result above, we have

$$\begin{aligned}\Sigma(\boldsymbol{k}, i\omega_n) = g^2\lambda \int \frac{d^2q}{(2\pi)^2} T \sum_{\Omega_m} & \frac{1}{q_y^2 + s + \dfrac{g^2|\Omega_m|}{2\pi v_F \kappa |q_y|}} \\ \times & \frac{1}{i(\Omega_m + i\omega_n) - v_F(k_x + q_x) - \kappa(k_y + q_y)^2/2 - \Sigma(i\Omega_m + i\omega_n)} \,. \end{aligned} \tag{93}$$

where we have dropped q_x in the boson propagator. We can now perform the integral over q_x, and observe that the expression is indeed independent of $\boldsymbol{k}$, and the frequency dependent Σ in the denominator. So we have our closed-form expression for the fermion self energy

$$\Sigma(i\omega_n) = -i\,\frac{g^2\lambda}{2v_F} \int \frac{dq_y}{2\pi} T \sum_{\Omega_m} \frac{\mathrm{sgn}(\omega_n + \Omega_m)}{q_y^2 + s + \dfrac{g^2|\Omega_m|}{2\pi v_F \kappa |q_y|}} \,. \tag{94}$$

We are interested in the singular behavior of this fermion self energy at the critical point $s = 0$. At $T > 0$, we have to account for thermal effects arising from the boson self-interaction u in (39) which make the renormalized s temperature dependent. We will not discuss these subtle issues [32–35] here, and limit ourselves below to $T = 0$.

For $s > 0$ and $T = 0$, evaluation of the integrals over q_y and Ω in (94) shows that $\mathrm{Im}\Sigma(\omega) \sim -(\omega/s)^2 \ln(1/|\omega|)$, which is the expected behavior for a two-dimensional Fermi liquid (see QPT

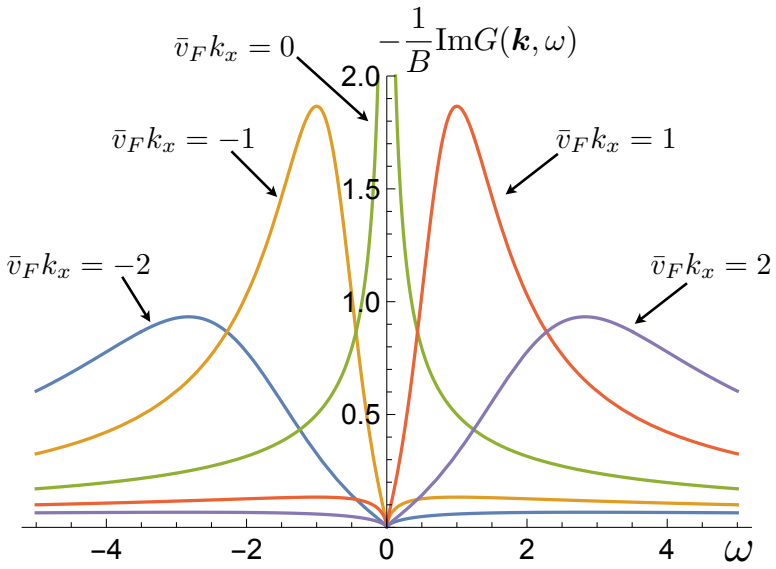

FIG. 17. Plot of fermion spectral density from (97) at wavevectors $\boldsymbol{k} = \boldsymbol{k}_0 + (k_x, 0)$ across the Fermi surface without quasiparticles. Here $\bar{v}_F = v_F/B$.

book). At the critical point $s = 0$, and at $T = 0$, we perform the q_y integral, and then the frequency integral to obtain

$$\begin{aligned}\Sigma(i\omega) &= -i\frac{g^2\lambda}{3v_F\sqrt{3}}\left(\frac{2\pi v_F\kappa}{g^2}\right)^{1/3}\int\frac{d\Omega}{2\pi}\frac{\mathrm{sgn}(\omega+\Omega)}{|\Omega|^{1/3}}\\ &= -iB\,\mathrm{sgn}(\omega)|\omega|^{2/3} \quad s=0, T=0\,,\end{aligned} \tag{95}$$

with

$$B = \frac{g^2\lambda}{2\pi v_F\sqrt{3}}\left(\frac{2\pi v_F\kappa}{g^2}\right)^{1/3}\,. \tag{96}$$

It is instructive to examine the frequency and momentum dependence of the $T = 0$ fermion Green's function across the Fermi surface. In the scaling limit, we can write the real frequency axis Green's function near the Fermi surface as

$$G(\boldsymbol{k},\omega) = \frac{1}{-v_F k_x - \kappa k_y^2/2 + iBe^{-i\pi\mathrm{sgn}(\omega)/3}|\omega|^{2/3}}\,. \tag{97}$$

As in the SYK model, we can drop the bare ω term in G^{-1} because it is subleading with respect to the frequency-dependent self energy. Note also the distinction in the singularity structure from that of the one-dimensional Tomonaga Luttinger liquid—the singularity here is entirely in the frequency dependence of the self energy, as in the SYK model. We show a plot of $-\mathrm{Im}G$ in Fig. 17. On the Fermi surface $k_x = 0$, $k_y = 0$ we have $\mathrm{Im}G \sim -1/|\omega|^{2/3}$, which is similar to the $\mathrm{Im}G \sim -1/|\omega|^{1/2}$ behavior of the SYK model. Unlike the Fermi liquid, there is no delta function in ω on the Fermi surface, indicating the absence of quasiparticles. Away from the Fermi surface,

ImG actually vanishes on the Fermi surface (see Fig. 17), and there is a broad spectral feature which disperses as $\omega = [(2v_F/(\sqrt{3}B))k_x]^{2/3}$. Note that the position of the Fermi surface is still given by the vanishing of the inverse Green's function at zero frequency, as in (25).

We can compute the momentum distribution function of the electrons from (97), and it leads to result similar in form to that of a Tomonaga-Luttinger liquid

$$n(\boldsymbol{k}) \sim -\mathrm{sgn}(v_F k_x + \kappa k_y^2/2)|v_F k_x + \kappa k_y^2/2|^{1/2} \,, \tag{98}$$

with a power-law singularity on the Fermi surface. But recall that the frequency dependent form of (97) is quite different from that for the one-dimensional electron gas.

At non-zero T, the SYK model displays simple ω/T scaling in its spectral function. There are 'quantum' contributions which do indeed scale as ω/T for the critical Fermi surface, but there are also additional corrections which arise from classical thermal fluctuations of ϕ which are important. So the $T > 0$ situation is rather complex [32–35], as we noted above.

B. Luttinger relation

The strong damping and breakdown of quasiparticles implied by (95) and (96) nevertheless does not remove the sharp Fermi surface. There is no singular momentum dependence in these expressions, and the frequency dependence still obeys (24). Consequently, there is still a Fermi surface specified by (25).

We now show that this Fermi surface obeys the same Luttinger relation as that of a Fermi liquid. The argument proceeds just as in Section I D. The evaluation of (35) proceeds as before, as the self energy all the needed properties. We only need to examine more carefully the fate of the Luttinger-Ward term in (31):

$$I_2 = -i \int_{-\infty}^{\infty} \int \frac{d^2k}{4\pi^2} \frac{d\omega}{2\pi} G(\boldsymbol{k}, i\omega) \frac{d}{d\omega} \Sigma(i\omega) e^{-i\omega 0^+} \,. \tag{99}$$

As the self energy of the critical Fermi surface is singular, it is possible that there is an anomalous contribution at $\omega = 0$ that leads to a non-vanishing I_2. However, that is not the case here because the singularity of the Green's function is much weaker as a result of its momentum dependence; the low energy Green's function is

$$G^{-1}(\boldsymbol{k}, i\omega) = -v_F k_x - \frac{\kappa}{2} k_y^2 - \Sigma(i\omega) \,, \tag{100}$$

and this diverges at $\omega = 0$ only on the Fermi surface $v_F k_x + \kappa k_y^2/2 = 0$. Indeed, with this form, the local density of states is a constant at the Fermi level. Consequently, there is no anomaly at $T = 0$, and $I_2 = 0$ from the Luttinger-Ward functional analysis. Incidentally, we note that the Luttinger-Ward functional in the large N limit is just the first term in the action I in Eq. (81), similar to the SYK model.

To complete this discussion, we add a few remarks on the structure of the Luttinger-Ward functional, and its connection to global U(1) symmetries [2, 3]. Consider the general case where there are multiple Green's functions (of bosons or fermions) $G_\alpha(k_\alpha, \omega_\alpha)$. Let the α'th particle have a charge q_α under a global U(1) symmetry. Then for each such U(1) symmetry, the Luttinger-Ward functional will obey the identity

$$\Phi_{LW}\left[G_\alpha(\boldsymbol{k}_\alpha, \omega_\alpha)\right] = \Phi_{LW}\left[G_\alpha(\boldsymbol{k}_\alpha, \omega_\alpha + q_\alpha \Omega)\right]. \tag{101}$$

Here, we are regarding Φ_{LW} as functional of two distinct sets of functions $f_{1,2\alpha}(\omega_\alpha)$, with $f_{1\alpha}(\omega_\alpha) \equiv G_\alpha(k_\alpha, \omega_\alpha + q_\alpha\Omega)$ and $f_{2\alpha}(\omega) \equiv G_\alpha(k_\alpha, \omega_\alpha)$, and Φ_{LW} evaluates to the same value for these two sets of functions. Expanding (101) to first order in Ω, and integrating by parts, we establish the corresponding $I_2 = 0$.

C. Transport

The highly singular self energy in (95) suggests that there will be strong scattering of charge carriers, and hence a low T resistivity which is larger than the $\sim T^2$ resistivity of a Fermi liquid. Indeed, it was argued in an early work [36] that the resistivity $\sim T^{4/3}$; this is weaker than $\Sigma \sim T^{2/3}$, because of the $(1 - \cos(\theta))$ factor in the transport scattering time, for scattering by an angle θ, and the dominance of forward scattering.

However, this argument ignores the strong constraints placed by momentum conservation [37–41] in a theory of critical fluctuations which is described by a translationally invariant continuum field theory. If we set up an initial state at $t = 0$ with a non-zero current, such a state necessarily has a non-zero momentum, which will remain the same for $t > 0$. The current will decay to a non-zero value which maximizes the entropy subject to the constraint of a non-zero momentum. This non-zero current as $t \to \infty$ implies that the d.c. conductivity is actually infinite. These considerations are similar to those of 'phonon drag' [42, 43] leading to the absence of resistivity from electron-phonon scattering. In practice, phonon drag is observed only in very clean samples [44], because otherwise the phonons rapidly lose their momentum to impurities. But the electron-phonon coupling is weak, allowing for phonon-impurity interactions before there are multiple electron-phonon interactions. In contrast, for the critical Fermi surface, the fermion-boson coupling is essentially infinite because it leads to the breakdown of electronic quasiparticles. So the critical Fermi surface must be studied in the limit of strong drag, with vanishing d.c. resistivity in the critical theory.

More remarkable and subtle is the fact that the non-Fermi liquid structure of (95) also does *not* feed into the optical conductivity, which remains very similar to that of a Fermi liquid [45–50] with the form:

$$\sigma(\omega) \sim \frac{1}{-i\omega} + |\omega|^0 + \cdots \quad (\omega^{-2/3} \text{ term has vanishing co-efficient}) \tag{102}$$

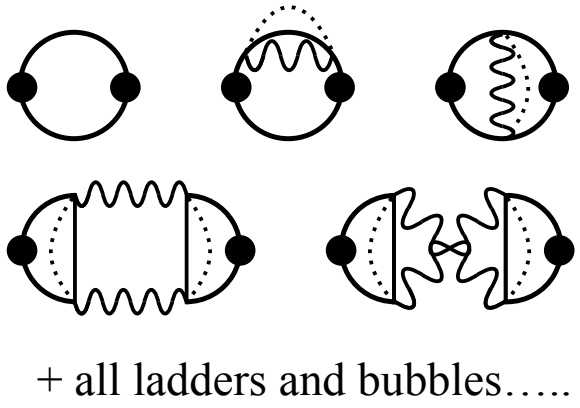

FIG. 18. Diagrams for the conductivity for the theory $\mathcal{L}_c + \mathcal{L}_v + \mathcal{L}_\phi$.

There has been a claim [51] of a $\omega^{-2/3}$ contribution to the conductivity, but its co-efficient vanishes after evaluation of all the graphs in Fig. 18 [48, 49]. This cancellation can be understood as a consequence of Kohn's theorem [52], which states that in a Galilean-invariant system only the first term of the right-hand-side of (102) is non-zero. A Galilean-invariant system is not considered here, but all contributions to the possible $\omega^{-2/3}$ term arise from long-wavelength processes in the vicinity of patches of the Fermi surface, and these patches can be embedded in a system which is Galilean-invariant also at higher energies.

VIII. UNIVERSAL THEORY OF STRANGE METALS: THE 2d-YSYK MODEL

See slides at https://sachdev.physics.harvard.edu/UQM24QCM.pdf.

Mechanisms extrinsic to the patch theory in Section VII A are required to relax the current and obtain a finite d.c. conductivity. In a system with strong interactions, such processes are most conveniently addressed by a 'memory matrix' approach that has been reviewed elsewhere [41]; this approach also has close connections to holographic approaches [53, 54]. Various mechanisms have been considered [38, 39, 55–58] involving spatial disorder or umklapp processes, and these do lead to a singular resistivity at low T. Here we focus on the results [48, 59, 60] obtained by including spatial disorder in Yukawa coupling.

We will add spatial disorder to the theory of Ising ferromagnetism in Section III, as described by the large N action in (76). We will not explicitly consider the models of quantum phase transitions in metals in Sections IV and V. The three cases in Sections III, IV, and V lead to distinct universality classes of quantum phase transitions in the clean limit. However, a remarkable fact is that the universality classes become the *same* once spatial disorder is included. This happens because: (i) the Fermi surface becomes 'fuzzy' because of elastic scattering, and constraints from momentum conservation become unimportant at distances larger than the fermion mean-free path,

and (ii) the boson propagator has the diffusive form in (105) in all three cases.

The most important source of spatial disorder in the theory of disordered Fermi liquids is potential scattering, and so it is natural to include that here in the present theory. A form amenable to the large N limit being described here is the random potential action, which we add to the action in (76)

$$\mathcal{S}_v = \frac{1}{\sqrt{N}} \sum_{\alpha,\beta=1}^{N} \int d^2r d\tau \, v_{\alpha\beta}(\boldsymbol{r}) \psi^\dagger_\alpha(\boldsymbol{r},\tau) \psi_\beta(\boldsymbol{r},\tau)$$
$$\overline{v_{\alpha\beta}(\boldsymbol{r})} = 0\,, \quad \overline{v^*_{\alpha\beta}(\boldsymbol{r}) v_{\gamma\delta}(\boldsymbol{r}')} = v^2\, \delta(\boldsymbol{r}-\boldsymbol{r}')\delta_{\alpha\gamma}\delta_{\beta\delta} \tag{103}$$

The solution of the corresponding large N saddle point equations shows [59] that the boson polarizibility in (92) is replaced by

$$\Pi(\boldsymbol{q}, i\Omega_n) \sim -\frac{g^2}{v^2}|\Omega_n|, \tag{104}$$

which leads to $z = 2$ behavior in the boson propagator, with

$$[D(\boldsymbol{q}, i\Omega_n)]^{-1} \sim q^2 + \gamma|\Omega_n|\,. \tag{105}$$

The corresponding fermion self energy is modified from (95): it a familiar elastic impurity scattering contribution Σ_v also present in a disordered Fermi liquid, along with an inelastic term Σ_g [48] with the 'marginal Fermi liquid' form [61]

$$\Sigma_v(i\omega_n) \sim -iv^2 \mathrm{sgn}(\omega_n), \quad \Sigma_g(i\omega_n) \sim -\frac{g^2}{v^2}\omega_n \ln(1/|\omega_n|)\,. \tag{106}$$

Despite the promising singularity in Σ_g, (106) does not translate [48] into interesting behavior in the transport: the scattering is mostly forward, and the resistivity is Fermi liquid-like with $\rho(T) = \rho(0) + AT^2$.

Much more interesting and appealing behavior results when we add spatial randomness in the Yukawa coupling. Such randomness will be generated by the potential randomness $v_{\alpha\beta}(x)$ considered above, but it has to included at the outset in the large N limit. More explicitly, we recall that the Yukawa coupling invariably arises from a Hubbard-Stratonovich decoupling of a four-fermion interaction: we can decouple such an interaction via a ϕ^2 term which is spatially uniform, and then all the spatial disorder is transferred to the Yukawa term.

We can also view spatial disorder in the Yukawa coupling as a form of 'Harris' disorder *i.e.* disorder in the local position of the quantum critical point. Such disorder is usually include as a spatially random contribution $\delta s(\boldsymbol{r})$ to the boson 'mass' s in (76). However, direct treatment of $\delta s(\boldsymbol{r})$ by the present large N method leads to unphysical results. We have argued [59] that random mass disorder should be treated exactly by rescaling ϕ so that the co-efficient of ϕ^2 is spatially independent. This rescaling induces spatial disorder in all other terms in (76), and the most relevant is the one in the Yukawa coupling.

So we *add* to the spatially independent Yukawa couplings $g_{\alpha\beta\gamma}$ in (76) a second coupling $g'_{\alpha\beta\gamma}(\boldsymbol{r})$ which has both spatial and flavor randomness with action

$$\mathcal{S}_{g'} = \frac{1}{N}\int d^2r d\tau\, g'_{\alpha\beta\gamma}(\boldsymbol{r})\psi^\dagger_\alpha(\boldsymbol{r},\tau)\psi_\beta(\boldsymbol{r},\tau)\phi_\gamma(\boldsymbol{r},\tau) \tag{107}$$
$$\overline{g'_{\alpha\beta\gamma}(\boldsymbol{r})} = 0\,, \quad \overline{g'^*_{\alpha\beta\gamma}(\boldsymbol{r})g'_{\delta\rho\sigma}(\boldsymbol{r}')} = g'^2\,\delta(\boldsymbol{r}-\boldsymbol{r}')\delta_{\alpha\delta}\delta_{\beta\rho}\delta_{\gamma\sigma}\,.$$

The complete action of the 2d-YSYK model is given by the sum of (76), (103), and (107). Then we obtain additional contributions to the boson and fermion self energies [59]

$$\Pi_{g'}(\boldsymbol{q}, i\Omega_n) \sim -g'^2|\Omega_n|\,, \quad \Sigma_{g'}(i\omega_n) \sim -ig'^2\omega_n \ln(1/|\omega_n|)\,. \tag{108}$$

Now the marginal Fermi liquid self energy does contribute significantly to transport [59], with a linear-T resistivity $\sim g'^2T$, while the residual resistivity is determined primarily by v. It is notable that it is the disorder in the interactions, v, which determines the slope of the linear-T resistivity, while it is the potential scattering disorder which determines the residual resistivity. Other attractive features of this theory are that it has an anomalous optical conductivity $\sigma(\omega)$ with $\mathrm{Re}[1/\sigma(\omega)] \sim \omega$ and a $T\ln(1/T)$ specific heat [59, 60].

---

[1] H. Bruus and K. Flensberg, *Many-Body Quantum Theory in Condensed Matter Physics: An Introduction*, Oxford Graduate Texts (OUP Oxford, 2004).

[2] S. Powell, S. Sachdev, and H. P. Büchler, *Depletion of the Bose-Einstein condensate in Bose-Fermi mixtures*, Phys. Rev. B **72**, 024534 (2005), cond-mat/0502299.

[3] P. Coleman, I. Paul, and J. Rech, *Sum rules and Ward identities in the Kondo lattice*, Phys. Rev. B **72**, 094430 (2005), cond-mat/0503001.

[4] M. Potthoff, *Non-perturbative construction of the Luttinger-Ward functional*, Condens. Mat. Phys **9**, 557 (2006), arXiv:cond-mat/0406671.

[5] A. Georges, O. Parcollet, and S. Sachdev, *Quantum fluctuations of a nearly critical Heisenberg spin glass*, Phys. Rev. B **63**, 134406 (2001), arXiv:cond-mat/0009388 [cond-mat.str-el].

[6] S. Sachdev, *Bekenstein-Hawking Entropy and Strange Metals*, Phys. Rev. X **5**, 041025 (2015), arXiv:1506.05111 [hep-th].

[7] A. Kitaev and S. J. Suh, *The soft mode in the Sachdev-Ye-Kitaev model and its gravity dual*, JHEP **05**, 183, arXiv:1711.08467 [hep-th].

[8] J. Maldacena and D. Stanford, *Remarks on the Sachdev-Ye-Kitaev model*, Phys. Rev. D **94**, 106002 (2016), arXiv:1604.07818 [hep-th].

[9] S. Sachdev and J. Ye, *Gapless spin-fluid ground state in a random quantum Heisenberg magnet*, Phys. Rev. Lett. **70**, 3339 (1993), arXiv:cond-mat/9212030 [cond-mat].

[10] O. Parcollet and A. Georges, *Non-Fermi-liquid regime of a doped Mott insulator*, Phys. Rev. B **59**, 5341 (1999), arXiv:cond-mat/9806119 [cond-mat.str-el].

[11] D. Chowdhury, A. Georges, O. Parcollet, and S. Sachdev, *Sachdev-Ye-Kitaev models and beyond: Window into non-Fermi liquids*, Rev. Mod. Phys. **94**, 035004 (2022), arXiv:2109.05037 [cond-mat.str-el].

[12] S. Sachdev, *Quantum Phases of Matter*, 1st ed. (Cambridge University Press, Cambridge, UK, 2023).

[13] J. S. Cotler, G. Gur-Ari, M. Hanada, J. Polchinski, P. Saad, S. H. Shenker, D. Stanford, A. Streicher, and M. Tezuka, *Black Holes and Random Matrices*, JHEP **05**, 118, [Erratum: JHEP 09, 002 (2018)], arXiv:1611.04650 [hep-th].

[14] D. Bagrets, A. Altland, and A. Kamenev, *Power-law out of time order correlation functions in the SYK model*, Nucl. Phys. B **921**, 727 (2017), arXiv:1702.08902 [cond-mat.str-el].

[15] D. Stanford and E. Witten, *Fermionic Localization of the Schwarzian Theory*, Journal of High Energy Physics **10**, 008 (2017), arXiv:1703.04612 [hep-th].

[16] Y. Gu, A. Kitaev, S. Sachdev, and G. Tarnopolsky, *Notes on the complex Sachdev-Ye-Kitaev model*, Journal of High Energy Physics **02**, 157 (2020), arXiv:1910.14099 [hep-th].

[17] W. Fu, D. Gaiotto, J. Maldacena, and S. Sachdev, *Supersymmetric Sachdev-Ye-Kitaev models*, Phys. Rev. D **95**, 026009 (2017), [Addendum: Phys.Rev.D 95, 069904 (2017)], arXiv:1610.08917 [hep-th].

[18] L. Pauling, *The Structure and Entropy of Ice and of Other Crystals with Some Randomness of Atomic Arrangement*, Journal of the American Chemical Society **57**, 2680 (1935).

[19] J. Maldacena, S. H. Shenker, and D. Stanford, *A bound on chaos*, JHEP **08**, 106, arXiv:1503.01409 [hep-th].

[20] J. Murugan, D. Stanford, and E. Witten, *More on Supersymmetric and 2d Analogs of the SYK Model*, JHEP **08**, 146, arXiv:1706.05362 [hep-th].

[21] A. A. Patel and S. Sachdev, *Critical strange metal from fluctuating gauge fields in a solvable random model*, Phys. Rev. B **98**, 125134 (2018), arXiv:1807.04754 [cond-mat.str-el].

[22] E. Marcus and S. Vandoren, *A new class of SYK-like models with maximal chaos*, JHEP **01**, 166, arXiv:1808.01190 [hep-th].

[23] Y. Wang, *Solvable Strong-coupling Quantum Dot Model with a Non-Fermi-liquid Pairing Transition*, Phys. Rev. Lett. **124**, 017002 (2020), arXiv:1904.07240 [cond-mat.str-el].

[24] I. Esterlis and J. Schmalian, *Cooper pairing of incoherent electrons: an electron-phonon version of the Sachdev-Ye-Kitaev model*, Phys. Rev. B **100**, 115132 (2019), arXiv:1906.04747 [cond-mat.str-el].

[25] Y. Wang and A. V. Chubukov, *Quantum Phase Transition in the Yukawa-SYK Model*, Phys. Rev. Res. **2**, 033084 (2020), arXiv:2005.07205 [cond-mat.str-el].

[26] E. E. Aldape, T. Cookmeyer, A. A. Patel, and E. Altman, *Solvable theory of a strange metal at the breakdown of a heavy Fermi liquid*, Phys. Rev. B **105**, 235111 (2022), arXiv:2012.00763 [cond-mat.str-el].

[27] W. Wang, A. Davis, G. Pan, Y. Wang, and Z. Y. Meng, *Phase diagram of the spin-1/2 Yukawa-Sachdev-Ye-Kitaev model: Non-Fermi liquid, insulator, and superconductor*, Phys. Rev. B **103**, 195108 (2021), arXiv:2102.10755 [cond-mat.str-el].

[28] D. Valentinis, G. A. Inkof, and J. Schmalian, *Correlation between phase stiffness and condensation energy across the non-Fermi to Fermi-liquid crossover in the Yukawa-Sachdev-Ye-Kitaev model on a lattice*, arXiv e-prints 10.48550/arXiv.2302.13134 (2023), arXiv:2302.13134 [cond-mat.supr-con].

[29] D. Valentinis, G. A. Inkof, and J. Schmalian, *BCS to incoherent superconductivity crossovers in the Yukawa-SYK model on a lattice*, arXiv e-prints 10.48550/arXiv.2302.13138 (2023), arXiv:2302.13138 [cond-mat.supr-con].

[30] H. Hosseinabadi, S. P. Kelly, J. Schmalian, and J. Marino, *Thermalization of Non-Fermi Liquid Electron-Phonon Systems: Hydrodynamic Relaxation of the Yukawa-SYK Model*, arXiv e-prints 10.48550/arXiv.2306.03898 (2023), arXiv:2306.03898 [cond-mat.str-el].

[31] I. Esterlis and J. Schmalian, *Cooper pairing of incoherent electrons: an electron-phonon version of the Sachdev-Ye-Kitaev model*, Phys. Rev. B **100**, 115132 (2019), arXiv:1906.04747 [cond-mat.str-el].

[32] E. E. Aldape, T. Cookmeyer, A. A. Patel, and E. Altman, *Solvable theory of a strange metal at the breakdown of a heavy Fermi liquid*, Phys. Rev. B **105**, 235111 (2022), arXiv:2012.00763 [cond-mat.str-el].

[33] I. Esterlis, H. Guo, A. A. Patel, and S. Sachdev, *Large N theory of critical Fermi surfaces*, Phys. Rev. B **103**, 235129 (2021), arXiv:2103.08615 [cond-mat.str-el].

[34] J. A. Damia, M. Solís, and G. Torroba, *How non-Fermi liquids cure their infrared divergences*, Phys. Rev. B **102**, 045147 (2020), arXiv:2004.05181 [cond-mat.str-el].

[35] Y. Wang, A. Abanov, B. L. Altshuler, E. A. Yuzbashyan, and A. V. Chubukov, *Superconductivity near a Quantum-Critical Point: The Special Role of the First Matsubara Frequency*, Phys. Rev. Lett. **117**, 157001 (2016), arXiv:1606.01252 [cond-mat.supr-con].

[36] P. A. Lee, *Gauge field, Aharonov-Bohm flux, and high-T_c superconductivity*, Phys. Rev. Lett. **63**, 680 (1989).

[37] S. A. Hartnoll, P. K. Kovtun, M. Muller, and S. Sachdev, *Theory of the Nernst effect near quantum phase transitions in condensed matter, and in dyonic black holes*, Phys. Rev. B **76**, 144502 (2007), arXiv:0706.3215 [cond-mat.str-el].

[38] D. L. Maslov, V. I. Yudson, and A. V. Chubukov, *Resistivity of a Non-Galilean-Invariant Fermi Liquid near Pomeranchuk Quantum Criticality*, Phys. Rev. Lett. **106**, 106403 (2011), arXiv:1012.0069 [cond-mat.str-el].

[39] S. A. Hartnoll, R. Mahajan, M. Punk, and S. Sachdev, *Transport near the Ising-nematic quantum critical point of metals in two dimensions*, Phys. Rev. **B89**, 155130 (2014), arXiv:1401.7012 [cond-mat.str-el].

[40] A. Eberlein, I. Mandal, and S. Sachdev, *Hyperscaling violation at the Ising-nematic quantum critical*

point in two dimensional metals, Phys. Rev. B **94**, 045133 (2016), arXiv:1605.00657 [cond-mat.str-el].

[41] S. A. Hartnoll, A. Lucas, and S. Sachdev, *Holographic quantum matter*, MIT Press, Cambridge MA (2016), arXiv:1612.07324 [hep-th].

[42] R. Peierls, *Zur Theorie der elektrischen und thermischen Leitfähigkeit von Metallen*, Annalen der Physik **396**, 121 (1930).

[43] R. Peierls, *Zur Frage des elektrischen Widerstandsgesetzes für tiefe Temperaturen*, Annalen der Physik **404**, 154 (1932).

[44] C. W. Hicks, A. S. Gibbs, A. P. Mackenzie, H. Takatsu, Y. Maeno, and E. A. Yelland, *Quantum Oscillations and High Carrier Mobility in the Delafossite $PdCoO_2$*, Phys. Rev. Lett. **109**, 116401 (2012), arXiv:1207.5402 [cond-mat.str-el].

[45] H. K. Pal, V. I. Yudson, and D. L. Maslov, *Resistivity of non-Galilean-invariant Fermi- and non-Fermi liquids*, Lithuanian Journal of Physics and Technical Sciences **52**, 142 (2012), arXiv:1204.3591 [cond-mat.str-el].

[46] D. L. Maslov and A. V. Chubukov, *Optical response of correlated electron systems*, Reports on Progress in Physics **80**, 026503 (2017), arXiv:1608.02514 [cond-mat.str-el].

[47] A. V. Chubukov and D. L. Maslov, *Optical conductivity of a two-dimensional metal near a quantum critical point: The status of the extended Drude formula*, Phys. Rev. B **96**, 205136 (2017), arXiv:1707.07352 [cond-mat.str-el].

[48] H. Guo, A. A. Patel, I. Esterlis, and S. Sachdev, *Large-N theory of critical Fermi surfaces. II. Conductivity*, Phys. Rev. B **106**, 115151 (2022), arXiv:2207.08841 [cond-mat.str-el].

[49] Z. D. Shi, D. V. Else, H. Goldman, and T. Senthil, *Loop current fluctuations and quantum critical transport*, SciPost Phys. **14**, 113 (2023), arXiv:2208.04328 [cond-mat.str-el].

[50] H. Guo, D. Valentinis, J. Schmalian, S. Sachdev, and A. A. Patel, *Cyclotron resonance and quantum oscillations of critical Fermi surfaces*, arXiv e-prints , arXiv:2308.01956 (2023), arXiv:2308.01956 [cond-mat.str-el].

[51] Y. B. Kim, A. Furusaki, X.-G. Wen, and P. A. Lee, *Gauge-invariant response functions of fermions coupled to a gauge field*, Phys. Rev. B **50**, 17917 (1994), arXiv:cond-mat/9405083 [cond-mat].

[52] W. Kohn, *Cyclotron Resonance and de Haas-van Alphen Oscillations of an Interacting Electron Gas*, Phys. Rev. **123**, 1242 (1961).

[53] A. Lucas, *Conductivity of a strange metal: from holography to memory functions*, JHEP **03**, 071, arXiv:1501.05656 [hep-th].

[54] A. Lucas and S. Sachdev, *Memory matrix theory of magnetotransport in strange metals*, Phys. Rev. **B91**, 195122 (2015), arXiv:1502.04704 [cond-mat.str-el].

[55] A. A. Patel and S. Sachdev, *DC resistivity at the onset of spin density wave order in two-dimensional metals*, Phys. Rev. **B90**, 165146 (2014), arXiv:1408.6549 [cond-mat.str-el].

[56] X. Wang and E. Berg, *Scattering mechanisms and electrical transport near an Ising nematic quantum*

critical point, Phys. Rev. B **99**, 235136 (2019), arXiv:1902.04590 [cond-mat.str-el].

[57] D. V. Else and T. Senthil, *Strange Metals as Ersatz Fermi Liquids*, Phys. Rev. Lett. **127**, 086601 (2021), arXiv:2010.10523 [cond-mat.str-el].

[58] P. A. Lee, *Low-temperature T -linear resistivity due to umklapp scattering from a critical mode*, Phys. Rev. B **104**, 035140 (2021), arXiv:2012.09339 [cond-mat.str-el].

[59] A. A. Patel, H. Guo, I. Esterlis, and S. Sachdev, *Universal theory of strange metals from spatially random interactions*, Science **381**, 6659 (2023), arXiv:2203.04990 [cond-mat.str-el].

[60] C. Li, D. Valentinis, A. A. Patel, H. Guo, J. Schmalian, S. Sachdev, and I. Esterlis, *Strange metal and superconductor in the two-dimensional Yukawa-Sachdev-Ye-Kitaev model*, (2024), arXiv:2406.07608 [cond-mat.str-el].

[61] C. M. Varma, P. B. Littlewood, S. Schmitt-Rink, E. Abrahams, and A. E. Ruckenstein, *Phenomenology of the normal state of Cu-O high-temperature superconductors*, Phys. Rev. Lett. **63**, 1996 (1989).